

Remote Impact on Tropical Atlantic Climate Variability: Statistical Assessment and Dynamic Assessment*

Z. LIU

Center for Climatic Research/GN-IES, University of Wisconsin—Madison, Madison, Wisconsin

Q. ZHANG

State Key Laboratory of Atmospheric Sciences and Geophysical Fluid Dynamics, Institute of Atmospheric Physics, Chinese Academy of Sciences, Beijing, China

L. WU

Center for Climatic Research/GN-IES, University of Wisconsin—Madison, Madison, Wisconsin

(Manuscript received 27 March 2003, in final form 3 July 2003)

ABSTRACT

The remote impact of tropical Pacific and North Atlantic climate forcing on the tropical Atlantic sea surface temperature variability is assessed using both a traditional statistical correlation method and a model-aided dynamic method. Consistently, both assessment methods suggest that the remote impact contributes to nearly half of the variance of the tropical Atlantic sea surface temperature variability at interannual and decadal time scales. In the meantime, the other half of the sea surface temperature variability is generated predominantly in the tropical Atlantic climate system, with local ocean–atmosphere coupling playing a critical role. Furthermore, the leading sea surface temperature variability modes seem also to originate predominantly internally in the tropical Atlantic climate system. The main effect of the remote impact is therefore an enhancement of the variance of these variability modes. This model study also shows some differences between the statistical and dynamic assessment methods, which may have implications on the methodology of the assessment as well as the dynamics of the system.

1. Introduction

It has long been recognized that the El Niño–Southern Oscillation (ENSO) can exert a significant impact on the interannual variability over the tropical North Atlantic (e.g., Covey and Hastenrath 1978; Curtis and Hastenrath 1995; Enfield and Mayer 1997; Ruiz-Barradas et al. 2000; Czaja et al. 2002; Wu et al. 2002; Huang et al. 2002) via the anomalous atmospheric Walker circulation (Klein et al. 1999; Saravanan and Chang 2000; Chiang et al. 2000) and the Pacific–North American (PNA) atmospheric teleconnection (Nobre and Shukla 1996). It has also been suggested that tropical Pacific sea surface temperature (SST) variability affects interannual (Covey and Hastenrath 1978; Latif and Barnett

1995; Latif and Grotzner 2000) and decadal (Latif 2000; Chiang et al. 2000) climate variability in the equatorial Atlantic Ocean. Similarly, North Atlantic climate variability has also been found to have a significant impact on the tropical North Atlantic through the oceanic (Hansen and Bezdek 1996; Yang 1999; Malanotte-Rizzoli et al. 2000), atmospheric (Nobre and Shukla 1996; Seager et al. 2000; Czaja et al. 2002; Wu and Liu 2002), and coupled ocean–atmosphere (Xie and Tanimoto 1998) processes. It is therefore well established that a significant part of tropical Atlantic variability (TAV) is contributed by remote climate forcing (see Marshall et al. 2001 for a review).

In spite of these studies, the remote impact on the tropical Atlantic still needs to be better quantified and understood. In particular, all the previous studies have used a statistical assessment method to estimate the remote impact. The explained variance by the remote forcing [ENSO or North Atlantic Oscillation (NAO)] is defined as the squared (maximum lagged) correlation between the tropical Atlantic SST anomaly (SSTA) and

* Center for Climatic Research Contribution Number 820.

Corresponding author address: Z. Liu, Center for Climatic Research, 1225 W. Dayton St., Madison, WI 53706.
E-mail: zliu3@wisc.edu

the forcing index. For example, the monthly Niño-3 (5°S – 5°N , 150° – 90°W) SST anomaly (SSTA), as the index for ENSO, has a maximum correlation with the tropical North Atlantic SSTA of 0.5 with the index leading by about one season. This implies that ENSO explains about $(0.5)^2 = 25\%$ of the SSTA variance in the tropical North Atlantic (e.g., Enfield and Mayer 1997; Ruiz-Barradas et al. 2000; Czaja et al. 2002). This traditional statistical assessment method has been used widely for climate studies. This method for extracting the impact of climate forcing can be shown correct for some forced systems (e.g., appendix A). However, for a complex system such as the coupled ocean–atmosphere system, and the resulting SST variability, is this statistical method correct, quantitatively or even qualitatively? This question is impossible to clarify from observations alone, because the true remote impact can be obtained only with controlled grand geophysical experiments that are not feasible in the real world. However, in the context of a climate model, this question can be clarified. Specifically designed sensitivity model experiments can single out the effect of each climate forcing, providing a dynamic assessment of the impact of the corresponding forcing. The dynamic assessment can also be used to evaluate the statistical assessment. The major contribution of this paper is to present the first model-aided dynamic assessment of the remote impact on TAV as well as a comparison of this method with the traditional statistical method. Some preliminary results on the dynamic assessment have been reported previously (Wu and Liu 2002; Wu et al. 2002).

The remote impact on tropical Atlantic SSTA is assessed using the traditional statistical method as well as a model-aided dynamic method. Two comparison strategies are also used. We will first compare the statistical assessment in both observations and the model control simulation, and then compare the statistical assessment and the dynamic assessment in the model. The first comparison provides information of the model performance while the second comparison provides information on the two assessment methods. It is found that the two assessment methods are largely consistent and both identify a significant remote impact from the tropical Pacific and North Atlantic SSTA, with the combined remote impact explaining nearly half of the total SSTA variance. The statistical assessment, nevertheless, tends to underestimate the remote impact for seasonal and interannual variability. Our study also demonstrates that the other half of the TAV variance is generated primarily locally within the tropical Atlantic climate system, with ocean–atmosphere coupling playing an important role. The paper is arranged as follows. Section 2 introduces the data and model. Section 3 assesses the remote impact statistically for both observations and the control simulation of the coupled model. Section 4 assesses the remote impact dynamically in the coupled model using sensitivity experiments and compares the dynamic as-

essment with the statistical assessment. Further discussions of the role of local ocean–atmosphere coupling and North Atlantic atmospheric variability are given in section 5. A summary and further discussions are given in section 6.

2. Data and model

The observational analyses use the Global Sea Ice and Sea Surface Temperature dataset (GISST) SSTs (Parker et al. 1995) from 1903 to 1994 and the sea level pressure (SLP) from the Comprehensive Ocean–Atmosphere Data Set (COADS; da Silva et al. 1994) for 1945–93. All the data, including the model output discussed later, are first seasonally averaged and detrended. This “seasonal” data will be used to represent total variability. For interannual (roughly 1–7 yr) and decadal (roughly >7 yr) variability, we first derive the “annual” data with a 5-season running mean of the seasonal data; we then derive the “decadal” variability data with a low-pass filter [two consecutive 13-season running-means; this kind of filter yields smaller Gibbrian overshoots and sidelobes in the frequency response function (Zhang et al. 1997)] of the annual data; we finally obtain the “interannual” variability data as the difference between the annual data and the decadal variability data.

The model is the Fast Ocean Atmosphere Model (FOAM; Jacob 1997). FOAM is a fully coupled ocean–atmosphere model without flux adjustment. The atmospheric component of FOAM is a fully parallel version of the National Center for Atmospheric Research (NCAR) Community Climate Model 2 (CCM2), in which the atmospheric physics are replaced by those of CCM3. The atmospheric component has R15 resolution (equivalent grid spacing of about $4.5^{\circ} \times 7.5^{\circ}$ latitude–longitude). The ocean component was developed following the Geophysical Fluid Dynamics Laboratory (GFDL) Modular Ocean Model (MOM) with a resolution of 1.4° latitude \times 2.8° longitude \times 16 levels. The coupled FOAM simulations are integrated for about 400 yr starting from the 456th year of a long control simulation. The upper ocean and the atmosphere reached a quasi-equilibrium in the first few decades and therefore the data of the last 350 yr are used for analysis (Table 1).

FOAM captures most major features of the observed tropical climatology (Jacob 1997; Liu et al. 2003), as in most other state-of-the-art climate models. The simulated climatology resembles broadly those of the NCAR Climate System Model (CSM; Boville and Gent 1998; Otto-Bliesner and Brady 2001). FOAM also produces a reasonably realistic ENSO (Liu et al. 2000) and Pacific decadal variability (Liu et al. 2002), although the simulated variability is somewhat weaker than in observations.

The most serious model deficiency of tropical climatology is the tendency of a double intertropical con-

TABLE 1. Explained variances due to the remote impact from the tropical Pacific (column 2), North Atlantic (column 3), combined tropical Pacific and North Atlantic (column 4), and the South Atlantic (column 5) averaged over the northern (NTA, 5°–25°N, 70°–20°W), equatorial (ETA, 5°S–5°N, 40°W–10°E), and southern (STA, 5°–25°S, 40°W–0°) tropical Atlantic for (a) total, (b) interannual, and (c) decadal variability. Each remote impact is estimated with the statistical assessment of observations (OB) and the model CTRL (CT), as well as the dynamic assessment of the model (DY). The tropical Pacific, North Atlantic, and South Atlantic impact used the SSTA indices TP-SST (10°S–10°N, 130°E–80°W), NA-SST (40°–60°N, 70°W–0°E) and SA-SST (30°–50°S, 70°W–20°E), respectively. The combined impact of two remote forcings in the statistical analysis used multiregression. The dynamic assessment is the same in columns 3 and 5, because both the North Atlantic and South Atlantic impacts use the same experiment PBC_ET. (A parenthesis indicates a physically unlikely impact.)

	Tropical Pacific			N. Atlantic			TP + NA			S. Atlantic		
	OB	CT	DY	OB	CT	DY	OB	CT	DY	OB	CT	DY
(a) Total variability												
NTA	21	18	20	19	5	30	38	22	40	4	1	(30)
ETA	6	16	24	6	1	16	12	16	36	4	1	16
STA	10	33	38	2	1	(21)	11	33	(45)	6	1	21
(b) Interannual variability												
NTA	44	36	39	15	4	37	50	37	52	13	5	(37)
ETA	11	29	35	7	1	24	14	29	40	14	2	24
STA	28	58	58	7	2	(34)	33	58	(66)	20	1	34
(c) Decadal variability												
NTA	13	6	6	47	29	56	51	37	58	8	10	(56)
ETA	8	27	31	36	8	4	39	36	52	8	18	4
STA	12	37	48	15	2	(36)	24	41	(66)	10	17	36

vergence zone (ITCZ), with the ITCZ in boreal winter migrating into the Southern Hemisphere in FOAM, instead of staying north of the equator as in observations (see Fig. 1 of Liu et al. 2003). This model deficiency is common among coupled GCMs. Specifically, in the tropical Atlantic region, the seasonal climatology of surface winds in the control simulation (CTRL) resemble closely the observations in boreal summer and fall, both converging towards the ITCZ between 5° and 10°N. The model winds, however, penetrate across the equator converging toward 5° to 10°S in boreal winter and spring, in contrast to the observational winds that converge toward the equator. The southward intrusion of the ITCZ distorts the climate variability, and in turn results in an unrealistic remote impact south of the equator, as will be seen later. Associated with this wind field, the seasonal cycle of equatorial Atlantic SST tends to be dominated by a semiannual component in the model, rather than an annual component in observations. The model has a cold center emerging in the western equatorial Atlantic in fall and winter, resulting in a cold tongue in the western Atlantic in the annual mean SST. This is opposite to the observation which has the cold tongue in the eastern equatorial Atlantic. This deficiency also appears to be common in many coupled models, including the NCAR CSM (Davey et al. 2002). Related to the model deficiency in the simulation of SST and surface winds, the equatorial thermocline also tends to be flatter and more diffusive in the model than in the observation. These model deficiencies should be kept in mind in later discussions of the TAV, especially for those features in the equatorial and tropical South Atlantic.

In spite of these model deficiencies, FOAM produces a reasonable TAV, comparable with some state-of-the-art coupled models (e.g., Latif and Grotzner 2000;

Huang et al. 2002). The two leading EOFs of the SSTA show a symmetric mode and a dipole mode (Liu and Wu 2000), consistent with observations (Hastenrath 1978; Houghton and Tourre, 1992). The leading rotated EOFs (REOFs) of SSTA also show strong similarity between observations CTRL (Fig. 1). The observational REOF1 (Fig. 1a1) is centered in the southeastern equatorial Atlantic near the Gulf of Guinea. The pattern of this equatorial Atlantic mode appears somewhat similar to the interannual Atlantic El Niño mode (Zebiak 1993; Ruiz-Barradas et al. 2000), but has a much stronger decadal characteristics in the observation (Enfield et al. 1999). The REOF2 (Fig. 1a2) is centered in the tropical North Atlantic, sometimes known as the tropical North Atlantic mode (Houghton and Tourre 1992; Enfield and Mayer 1997) and the REOF3 (Fig. 1a3) is centered in the southwestern tropical Atlantic against the Brazilian coast, representing a major mode of variability in the tropical South Atlantic. FOAM seems to reproduce all three modes (Figs. 1b1–1b3), although the order of some modes are altered. The tropical North Atlantic mode becomes the first REOF (Fig. 1b2) and the equatorial Atlantic mode appears as the third REOF. The major deficiency of the FOAM TAV is its second REOF, which is centered in the western equatorial Atlantic and has no counterparts in the observations (not shown). This western equatorial Atlantic mode appears to be caused by the deficient model equatorial seasonal cycle, and more specifically, the excessive southward migration of the ITCZ in boreal winter.

3. Statistical assessment: A maximum correlation estimate

To identify the remote impact on tropical Atlantic SSTA, one could use a statistical approach to obtain the

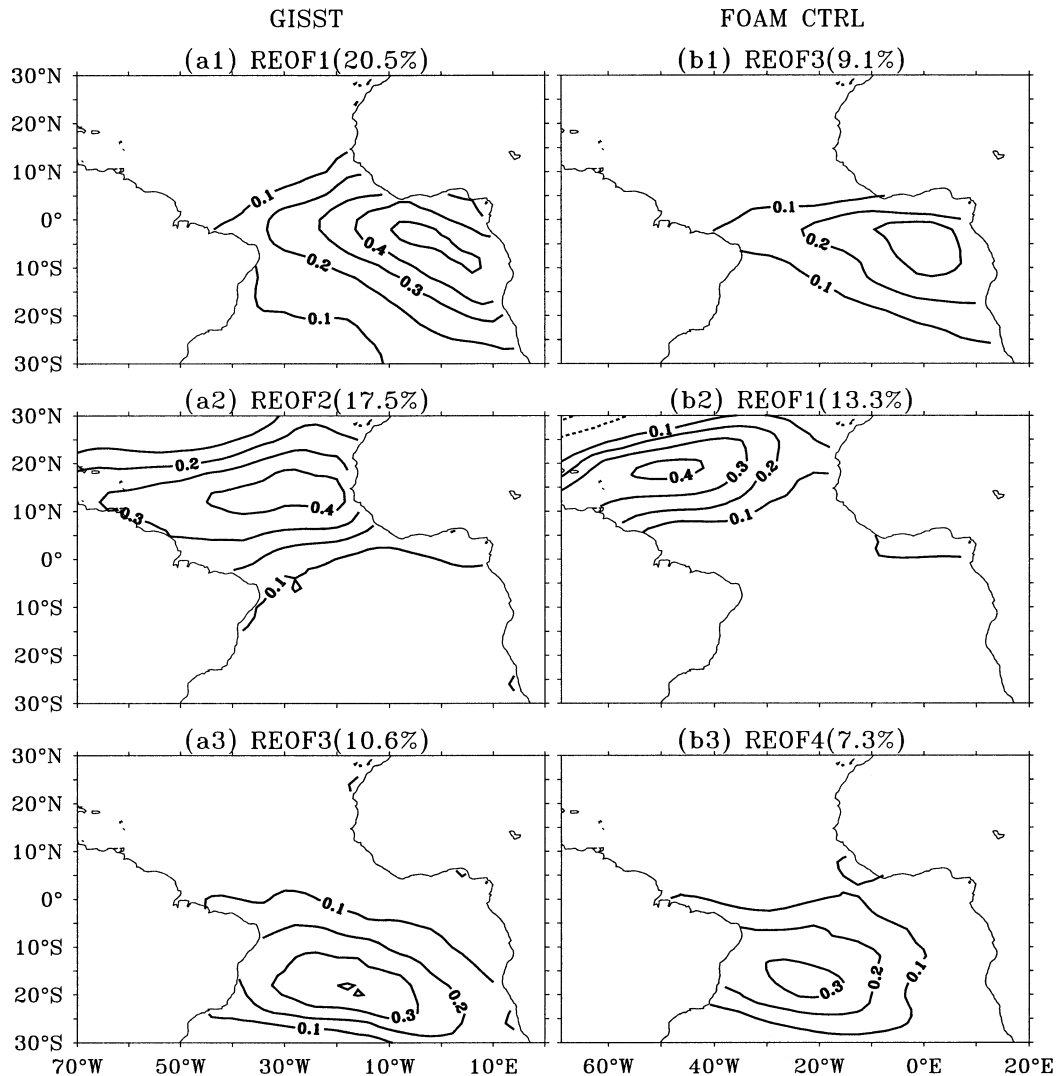


FIG. 1. The leading rotated EOF modes for tropical Atlantic SSTA in (a) observations (GISST 1903–94) and (b) the FOAM CTRL simulation. The data (in all the analyses here) are averaged for each season and the linear trend is removed prior to the analysis. The first 10 EOF modes are used for rotation to derive the REOF (using the varimax method). The REOF2 in CTRL (not shown) is centered in the western equatorial Atlantic and is caused by the deficient equatorial seasonal cycle of the model. The magnitude of each REOF is reflected in its pattern while its time series is normalized by the standard deviation.

maximum (magnitude of) correlation between the SSTA and forcing index; the square of this maximum correlation gives the explained variance of the forcing (see appendix A). Previous studies used a single-lag maximum correlation estimate, which selects the correlation field at a particular lag τ_0 such that the overall correlation with the forcing index is approximately maximum; the square of this correlation coefficient field at each grid point (x, y) is then used as the explained variance there:

$$\text{var}(T)(x, y) = [\text{cor}\langle T(x, y, t), \text{index}(t + \tau_0) \rangle]^2. \quad (3.1)$$

As a benchmark, we first calculate the correlation for both observations and the FOAM CTRL using the sea-

sonal data. For the remote impact from the tropical Pacific, we will use the SSTA averaged between 10°S and 10°N across the equatorial Pacific as the forcing index (TP-SST). Over the tropical North and South Atlantic, the SSTA tends to reach the maximum correlation with TP-SST with the SSTA lagging by about a season in observations (Fig. 2a). This feature is largely reproduced in the model (Fig. 2b). Therefore, the lag-1 correlation field ($\tau_0 = -1$ season) can be used as an approximate estimate of the explained variance of the tropical Pacific. The lag-1 correlation fields of observations (Fig. 3a) and the CTRL (Fig. 3b) show a general agreement, both being characterized by a double positive correlation maximum of about 0.4 near 20°N and 20°S. The

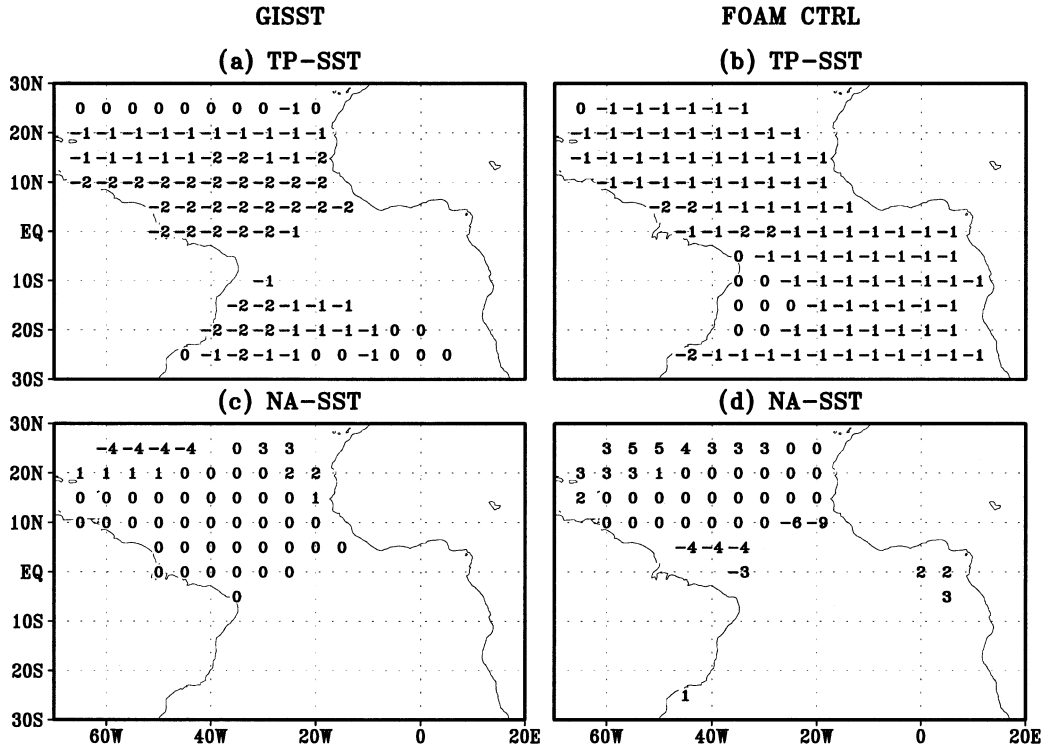


FIG. 2. The lead-lag (in season) at which the maximum correlation is achieved between the seasonal tropical Atlantic SSTA and the (a), (b) tropical Pacific SST index TP-SST and (c), (d) the North Atlantic SST index NA-SST in (a), (c) observations and (b), (d) CTRL. A negative lag means that the SSTA lags the index. Lags in the region of statistically insignificant correlation (<5%) are neglected.

correlations are statistically significant at the 99% level over most of the tropical Atlantic for both the model and observations, as indicated by the shading. The explained variance by the tropical Pacific impact, as inferred from the squared correlation, is therefore up to about 20%, consistent with previous results (Enfield and Mayer 1997; Ruiz-Barradas et al. 2000; Czaja et al. 2002). The model, however, overestimates the correlation in the southern tropical Atlantic and equatorial Atlantic, while it slightly underestimates the correlation in the northern tropical Atlantic. As a result, the model shows a Pacific influence stronger on the southern than on the northern tropical Atlantic, opposite to observations. In addition, the principal maximum and minimum of correlation is located closer to the equator in the model. These model-observation differences in the equatorial and tropical Atlantic are likely caused by the excessive southward migration of the model ITCZ, which allows the Pacific SSTA to affect the tropical Atlantic south of the equator, through the anomalous atmospheric Walker circulation, more effectively in the model than in observations.

The North Atlantic SSTA averaged between 40° and 60°N is used as the index of North Atlantic SST forcing (NA-SST). [An analysis with the standard NAO index using the sea level pressure (Hurrell 1995) is discussed

later in section 5]. The maximum correlation between NA-SST and the most part of the tropical North Atlantic SSTA occurs approximately simultaneously in both observations and the model (Figs. 2c,d). Therefore, the simultaneous correlation is used ($\tau_0 = 0$) as an approximation of the North Atlantic influence on the tropical Atlantic. This correlation is positive and confined in the tropical North Atlantic in both observations (Fig. 3c) and the model (Fig. 3d). The observation shows a positive correlation of over 0.4, corresponding to an explained variance of 20%, while the model has a positive correlation of 0.3, corresponding to an explained variance of 10%. The underestimation of the NA-SST influence in the model occurs predominantly for inter-annual variability, as will be seen later.

The earlier single-lag maximum correlation can be improved, because different regions achieve the maximum correlation at different lags, as seen in Fig. 2. Hereafter, we use the pointwise maximum correlation method. At each grid point (x, y), we find the maximum lagged correlation at lag $\tau_m(x, y)$ (e.g., Fig. 2 for total variability); the squared correlation gives the explained variance as

$$\text{var}(T)(x, y) = \{\text{cor}\langle T(x, y, t), \text{index}[t + \tau_m(x, y)] \rangle\}^2. \tag{3.2}$$

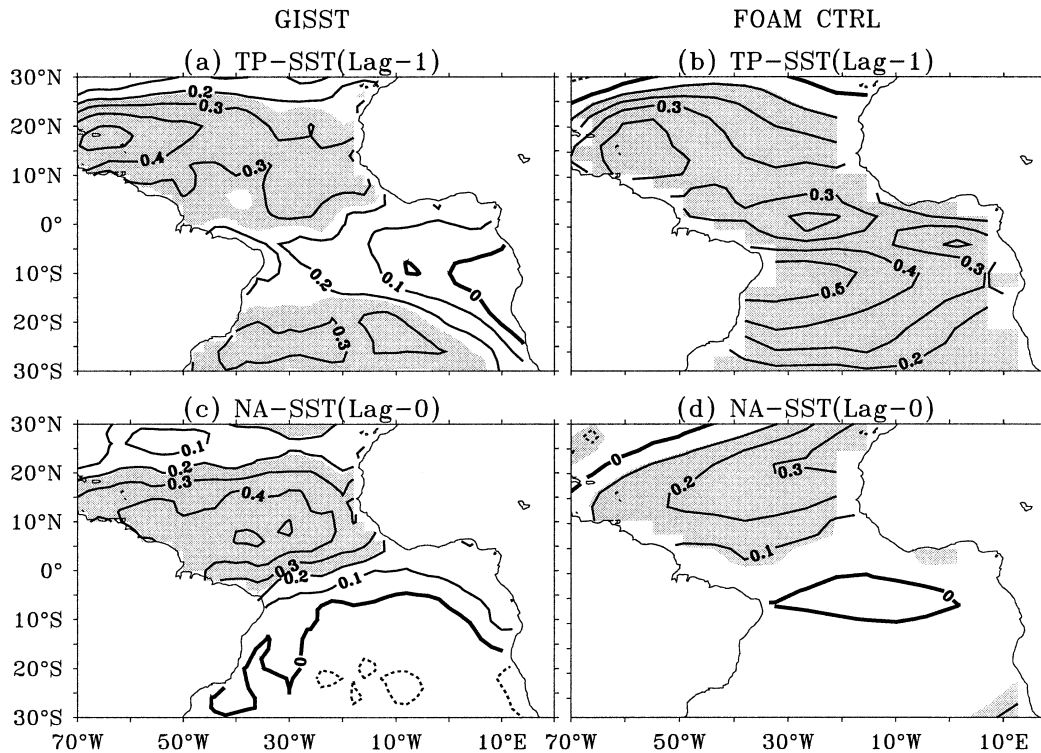


FIG. 3. The correlation coefficient field of the tropical Atlantic SSTA with (a), (b) the tropical Pacific SST index TP-SST (averaged in 10°S – 10°N and 130°E – 80°W), and (c), (d) the North Atlantic SST index NA-SST (averaged in 40° – 60°N and 70°W – 0°) in (a), (c) the GISST observations and (b), (d) FOAM CTRL. The correlation with TP-SST is done with the tropical Atlantic SST lagging by one season, and the correlation with the NA-SST is simultaneous. The shading indicates the 99% confidence level as determined by a local t test, for each point the effective sample size is calculated using the first-order autocorrelation (Dawdy and Matalas 1964), the obtained effective freedom is then used to determine the confidence band.

The pointwise maximum correlation provides the maximum possible forcing impact in the linear statistical sense.

The maximum correlation used for the statistical assessments, in both (3.1) and (3.2), should be limited to negative lags $\tau_m \leq 0$ if we want to extract the purely passive response (appendix A). We have not done so here because we want to include all the variability that is linearly related to the forcing, even including the part that is not a purely linear passive response. It turns out that the assessment of the pointwise maximum correlation (3.2) is not too much different from that of the single correlation (3.1), if we use the single lag as -1 for the tropical Pacific influence and 0 for North Atlantic influence (see Figs. B1 and B2 in appendix B).

In the following, we will use (3.2) to our interannual and interdecadal bandpass variability, because the explained variance defined in (3.2) [or (3.1)] can be applied directly to the bandpassed SST and forcing index. Therefore, all the explained variances estimated below are for the explained variances to the bandpass variances in the interannual and interdecadal bands, separately. This bandpass estimate is used here because we are mostly interested in the relative importance of the re-

mote forcing on TAV separately in the interannual and interdecadal bands, which are likely to be caused by different mechanisms because of the different time scales.¹

The statistic significance test is performed with the F test (von Storch and Zwiers 1999) on the ratio of the residual variance and the total (bandpass) variance. A significance of 95% means that the residual variance differ from the total variance at the 95% level, implying an explained remote impact significantly different from zero at the 95% level. For interannual variability the degree of freedom is adjusted as $n(1 - \rho_1^2)/(1 + \rho_1^2)$ with n being the number of total seasons and ρ_1 being the lag-1 autocorrelation coefficient. For decadal variability, the degree of freedom is chosen as 20 for the GISST observation and 60 for the model simulations, reflecting the low-pass filtering of approximately 6 yr.

¹ One can also estimate the explained variance to the total variance by multiplying each bandpass explained variance (e.g., in Figs. 4, 5, 6) with the ratio of the bandpass variance to the total variance. Averaged in the tropical Atlantic region, the ratio of the interannual and decadal variances to the total variance are about 25% and 30%, respectively, for the GISST, and about 20% and 15% respectively, for the CTRL simulation.

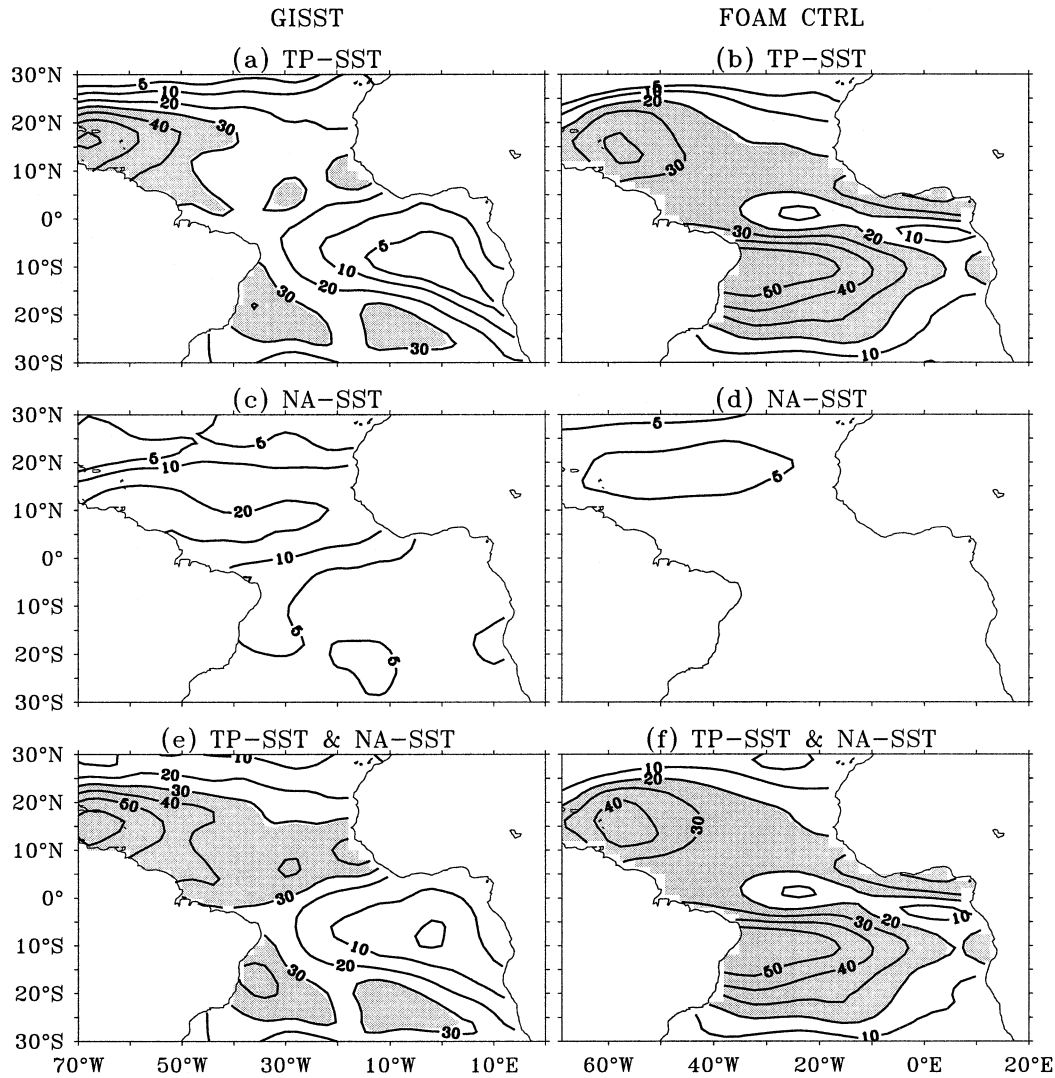


FIG. 4. Statistical assessment of the explained variances (%) of the interannual SST variability by (a), (b) tropical Pacific influence (TP-SST), (c), (d) North Atlantic influence (NA-SST) and (e), (f) their combination, in (a), (c), (e) observations and (b), (d), (f) the FOAM CTRL. The maximum pointwise correlation method in Eq. (3.2) is used with lead-lag searched in -12 to $+12$ seasons. The explained variance above 5 is significant at the 99% level. The contour interval is 10, with the additional contour of 5 also plotted. The combined effects in (e) and (f) are estimated by a multiple linear regression. The shading indicates the 95% confidence level as determined by an F test. The effective freedom is chosen as in Fig. 3.

Tropical Pacific impact is estimated using the pointwise maximum correlation method (3.2) for interannual (Fig. 4) and interdecadal (Fig. 5) variability. For interannual variability, the tropical Pacific influence reaches up to 50% and 40% in the observed northern and southwestern tropical Atlantic, respectively, (Fig. 4a), but up to 40% and over 50% in the model northern and southern tropical Atlantic, respectively, (Fig. 4b). These explained variances are statistically significant at the 95% level based on the F test. In both cases, the explained variances of interannual variability are substantially stronger than that for the total variability (the latter are similar to the squared correlation field in Figs. 3a,b).

For decadal variability, the explained variance by tropical Pacific influence (Figs. 5a,b) is smaller than the explained variance by the tropical Pacific for interannual variability, by a factor of about 2, and the explained decadal variance is not statistically significant. The overall larger explained variance of the tropical Pacific SST for interannual variability than for decadal variability implies that the interannual ENSO variability is particularly important for the interannual variability of TAV. This is consistent with other observational analyses (Cazja et al. 2002). Our correlation analysis of the tropical Pacific SSTA with the atmospheric pressure and wind fields show a clear signature of the anomalous

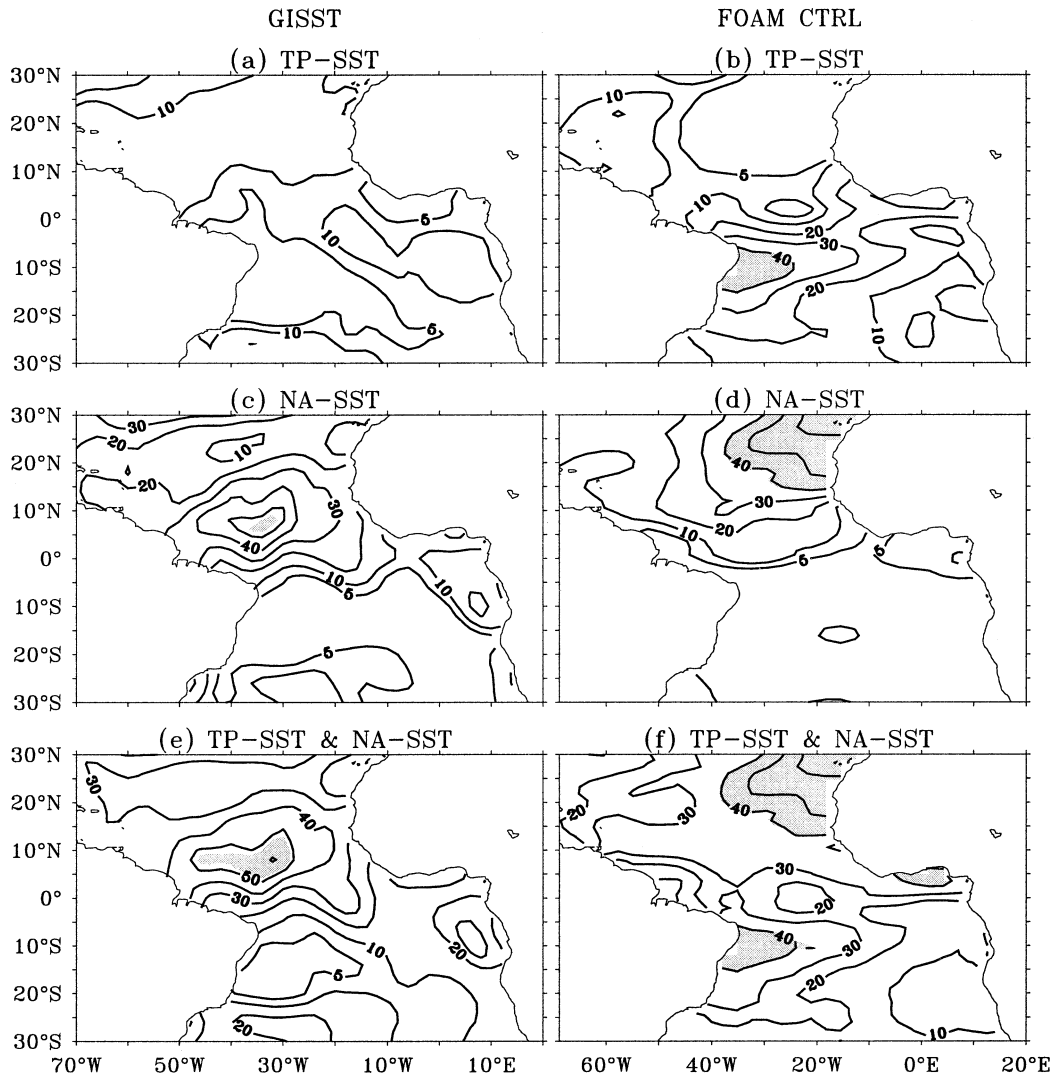


FIG. 5. The same as in Fig. 4 but for decadal variability. The maximum lead-lag searched is from -32 seasons to $+32$ seasons.

Walker circulation (not shown), which closely resembles that in Saravanan and Chang (2000). The major deficiency of the coupled model here, as discussed before regarding Fig. 3b, is a bias of stronger Pacific influence on the southern tropical Atlantic.

The North Atlantic SST explains up to 20% of interannual variability (Fig. 4c) and over 40% of decadal variability (Fig. 5c) in the observed tropical Atlantic SSTA. The North Atlantic SST impact is statistically insignificant for interannual variability, but marginally significant for decadal variability. In contrast to the tropical Pacific SST influence, the North Atlantic SST impact is stronger at decadal time scales. This stronger North Atlantic impact at decadal rather than interannual time scales is also simulated in the model (Figs. 4d, 5d). For reasons yet unclear, the North Atlantic SST impact, while comparable in the model and observations for

decadal variability (Figs. 5c,d), is much weaker in the model than in observations for interannual variability (Figs. 4c,d).

The combined influence of the tropical Pacific and North Atlantic, as estimated by a multiple linear regression against both the TP-SST and NA-SST, is roughly the sum of the two individual impacts in observations and the model (Figs. 4e,f and Figs. 5e,f). This occurs because the tropical Pacific SSTA is independent of the North Atlantic SSTA at all the time scales in observations and the model (with the correlation between TP-SST and NA-SST usually smaller than 0.05, insignificant at the 99% level).

The earlier assessment with the pointwise maximum correlation (3.2) is not too much different from that of the single correlation (3.1), if we use the single lag as -1 for the tropical Pacific influence and 0 for North

TABLE 2. FOAM experiments.

	PC domain	PB domain	Length
CTRL	None	None	350 yr
PC_TP	20°S–20°N Pacific	None	350 yr
PBC_ET	> 30° Atlantic, > 20° Pacific and Indian	Same as PC region	150 yr
PBC_TAV	Everywhere except for < 30° in the Atlantic	Same as PC region	350 yr
PC_G	Global ocean	None	350 yr

Atlantic influence (Figs. B1, B2). This reflects the fact that the tropical Atlantic SSTA is affected predominantly by the remote impact at these lags (as seen in Fig. 2) as a response to large-scale atmospheric forcing. It is interesting to compare the tropical Pacific impact with the North Atlantic impact. The former tends to lead the tropical Atlantic SSTA by about a season, while the latter tends to have a simultaneous correlation with the tropical Atlantic SSTA. The tropical Pacific influence is easier to understand because the SST responds to the surface heat flux with a lag of about a season (Czaja et al. 2002). In comparison, there is no time lag between the SSTA in the tropical and extratropical North Atlantic. This may suggest that the North Atlantic SSTA is not really a remote forcing for tropical North Atlantic SSTA. Instead, both SSTAs may be part of a gyrewide variation that either originates from a single mode of coupled variability, or is forced by something else, probably the atmospheric variability such as the North Atlantic Oscillation (NAO).

Finally, Table 1 summarizes the statistical assessment of various remote impacts on different regions of the tropical Atlantic Ocean. Overall, for total and interannual variability (Tables 1a, 1b), the tropical Pacific impact is comparable in observations and the model in the tropical North Atlantic, but the model tends to have a stronger impact on the equator and the tropical South Atlantic. The North Atlantic SST impact, however, is severely underestimated in the model. For decadal variability (Table 1c), the observation tends to have a stronger impact from both the tropical Pacific and North Atlantic on the tropical North Atlantic. For both interannual and decadal variability in the tropical North Atlantic, the combined explained variance of the two remote impacts is about 50% in observations and somewhat smaller, about 40%, in the model. The Pacific contribution is dominant for interannual variability, but the North Atlantic is dominant for decadal variability. This is consistent with previous works (Czaja et al. 2002). The impact on the equatorial Atlantic seems to be stronger in the model than in observations, which is likely to be related to the deficient equatorial seasonal climatology in the model.

4. Dynamic assessment: A modeling surgery estimate

The true remote impact in the model is identified in three sensitivity experiments (Table 2) using a modeling

surgery approach (Liu et al. 2002; Wu and Liu 2002; Wu et al. 2002, 2003). The effect of tropical Pacific SST is eliminated in the first experiment (PC_TP) by applying a partial coupling (PC) scheme over the tropical Pacific (<|20°|). In the PC region, the atmosphere is forced by the climatological seasonal cycle of the CTRL SST, while the ocean is still forced by the atmosphere through the coupler. As such, ocean and atmosphere are coupled actively only outside the tropical Pacific. The effect of extratropical Atlantic SST is suppressed in the second experiment (PBC_ET) with the PC applied poleward of 30° in the Atlantic. Furthermore, extratropical teleconnection through the oceanic (Hansen and Bezdek 1996; Yang 1999; Malanotte-Rizzoli et al. 2000) and coupled ocean–atmosphere (Xie and Tanimoto 1998) bridges are cut off using a partial blocking (PB) scheme in the model ocean poleward of 30° in the Atlantic. In the PB domain, ocean temperature and salinity are restored towards the seasonal cycle of the CTRL climatology from the surface to the bottom, such that no extratropical oceanic temperature and salinity anomalies can penetrate into the tropical Atlantic. Finally, the combined tropical Pacific/extratropical Atlantic effect is removed in the third experiment (PBC_TAV), which is designed the same as PBC_ET, but with the PC applied to the global ocean except for the tropical Atlantic Ocean.

The remote impact is assessed dynamically as follows. At each point (x, y), the difference of the SSTA variances between the control and sensitivity experiments $\Delta\text{var}(T) = \text{var}(T)|_{\text{CTRL}} - \text{var}(T)|_{\text{Sens}}$ is defined as the contribution of the corresponding remote impact. The explained variance is simply the ratio of this remote contribution with the total SSTA variance of the CTRL:

$$\text{var}(T)(x, y) = \Delta\text{var}(T)(x, y)/\text{var}(T)|_{\text{CTRL}}(x, y). \quad (4.1)$$

Different from the statistical assessment (3.2) or (3.1) that is always positive, the dynamic assessment (4.1) can be of either sign. A positive contribution implies an enhancement of local SST variability by the remote impact while a negative contribution implies a cancellation of local SST variability by the remote forcing. In a stable linear system, the external forcing tends to enhance the variance of local variability, corresponding to a positive contribution (e.g., appendix A). Similar to the statistic assessment, the statistic significance is performed with the F test on the ratio of the variances of the corresponding sensitivity PC experiment and the CTRL experiment.

The dynamic assessment of the tropical Pacific impact (CTRL – PC_TP) on interannual and decadal variability (Figs. 6a,e) can be readily compared with the corresponding statistical assessment (Figs. 4b, 5b). The tropical Pacific impact on the interannual variability shows a striking similarity in the two assessments (Fig. 4b versus Fig. 6a), with a double maximum in the northern and southern tropical western Atlantic centered at 15°N and 10°S. The two assessments even agree in some seemingly subtle features, such as the two regions of minimum in the central and eastern equatorial Atlantic and the minimums toward 30° in both hemispheres. As a first comparison of this kind, the strong similarity between the two independent assessments is both assuring and encouraging. It suggests that both methods are reasonable, at least in this case. The fact that the statistical assessment can truly extract the remote interannual Pacific impact may imply that the tropical Pacific acts largely as a remote forcing on a stable system, consistent with recent studies on the mechanism of interannual variability in the equatorial and northern tropical Atlantic (Zebiak 1993; Czaja et al. 2002). Our result is also consistent with an experiment in the Center for Ocean–Land–Atmosphere Studies (COLA) model (Huang et al. 2002), in which the suppression of Pacific SST variability results in a significant reduction of SST variability in the tropical Atlantic.

For decadal variability, the dynamic assessment (Fig. 6e) appears to be consistent with the statistical assessment (Fig. 5b) in not showing significant impact on the tropical North Atlantic. The center of maximum in the tropical South Atlantic is shifted from against the western boundary in the statistical assessment to the central ocean in the dynamic assessment. Overall, the two assessments for decadal variability are not as consistent as the interannual variability. This may imply a more complex mechanism of the Pacific influence on the tropical Atlantic at decadal time scales.

The dynamic assessment of the remote impact from the extratropical Atlantic SSTA (CTRL – PBC_ET) for interannual (Fig. 6b) and decadal (Fig. 6f) variability are compared with the statistical assessment of the North Atlantic SST impact in Figs. 4d and 5d, respectively. In the tropical North Atlantic, the two assessments have a modest similarity for decadal variability (Fig. 6f versus Fig. 5d), both being characterized by a maximum over 50% toward the northeastern subtropics and a minimum toward the equator. In comparison, the two methods differ significantly for interannual variability, with the dynamic assessment over 40% (Fig. 6b), but the statistical assessment of less than 10% (Fig. 4d). Therefore, relative to the dynamic assessment, the statistical assessment is a severe underestimation for interannual variability, but is of comparable magnitude for decadal variability. This may also imply different dynamics of the North Atlantic impact on tropical SSTA at different time scales. Opposite to the tropical Pacific influence, the two assessments of the North Atlantic influence are sim-

ilar for decadal variability but different for interannual variability. This may suggest a difference of the mechanisms of the two remote impacts. It should be pointed out that over the tropical South Atlantic, the remote impact is significant in the dynamic assessments (Figs. 6b,f), but insignificant in the statistical assessments (Figs. 4d, 5d). This strong remote impact on the tropical South Atlantic in the dynamic assessment comes from the extratropical South Atlantic, because of the suppression of the effect of the extratropical South Atlantic SSTA in PBC_ET.

The combined effect of the tropical Pacific and extratropical Atlantic influence is assessed dynamically as the difference of CTRL – PBC_TAV (Figs. 6c,g). Overall, the combined effect is the sum of the two individual impacts, as is the case of the statistical assessment. Therefore, both assessments support the notion of largely independent impacts from the tropical Pacific and the North Atlantic SSTA.

It is interesting to notice several overall differences between the two assessments. The dynamic assessment has regions of negative contribution, while the statistical assessment, by its definition, is always positive. The negative explained variance is seen most clearly for the dynamic assessment of the decadal variability near the equator for the Pacific (Fig. 6e) and extratropical Atlantic (Fig. 6f) influences. As discussed after (4.1), the region of negative explained variance implies a suppression by the remote impact on the SST variability there. Although the precise mechanism that contributes to this negative impact is unclear to us, the negative impact does imply that the remote impact is more complex than simply a linear passive response. Nevertheless, over most of the tropical Atlantic, especially for interannual variability, the dynamic assessment is predominantly positive. This supports the notion that over most of the region, the response to the remote forcing tends to be more like a passive response, especially for interannual variability.

The statistical assessment tends to underestimate the explained variance for interannual variability, relative to the dynamic assessment. For the interannual influence of the tropical Pacific, the maximum explained variances are about 40% and 50% in the northern and southern tropical Atlantic, respectively, in the statistical assessment (Fig. 4b), but over 40% and 60% in the corresponding dynamic assessment (Fig. 6a). Even more striking is the underestimation of the North Atlantic impact on tropical North Atlantic interannual variability: the statistical assessment gives a maximum explained variance of less than 10% (Fig. 4d), while the dynamic assessment exceeds 40% (Fig. 6b). The underestimation of the statistical assessment is seen more clearly in the area-averaged explained variances of the two assessments (Table 1). For total (Table 1a) and interannual (Table 1b) variability, the Pacific influence is about 10%–20% lower in the statistical assessment than in the dynamic assessment (except for the tropical South

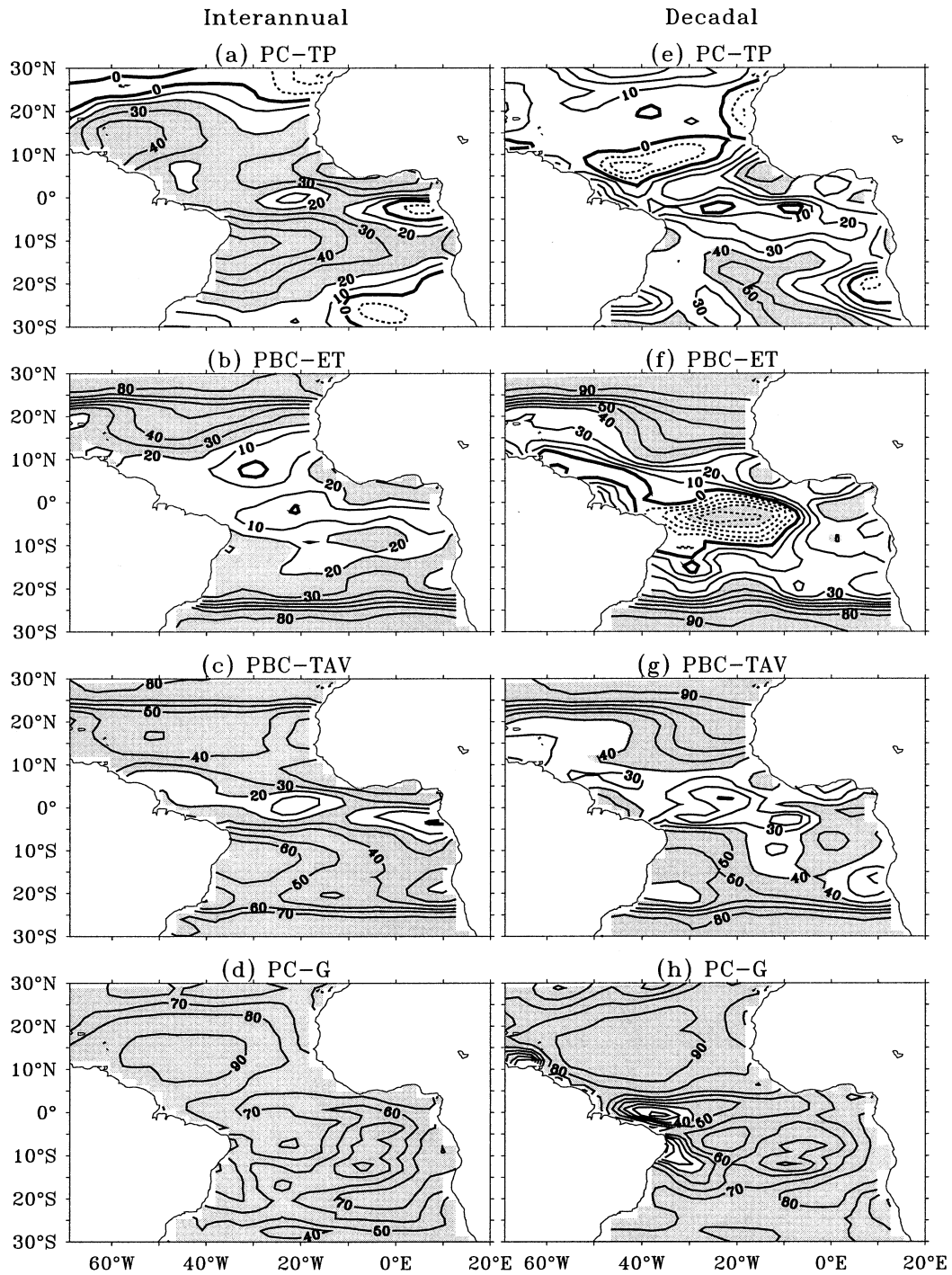


FIG. 6. Dynamic assessment of the explained variances (%) of tropical Atlantic SSTA using Eq. (4.1) for (a)–(d) interannual and (e)–(h) decadal variability. (a), (b) The impact of tropical Pacific SST using experiment PC-TP; (c), (d) the impact of extratropical Atlantic SST using experiment PBC-ET; (e), (f) the combined impact of tropical Pacific and extratropical Atlantic SST using experiment PBC-TAV; (g), (h) the additional impact of the local coupling using experiment PC-G. The contour interval is 10. Shading convention is the same as in Fig. 4.

Atlantic interannual variability); the North Atlantic impact is almost zero in statistical assessment, but 20% to 30% for the dynamic assessment.² In comparison, the statistical assessment of decadal variability does not seem to have a very systematic high or low bias relative to the dynamic assessment (Table 1c). It should also be noted that the dynamic assessment in the regional average may appear lower than the impression based on the regional maximums, partly because of the average of the negative contributions, especially for decadal variability (Figs. 6e,f).

The underestimation by the statistical assessment appears to be, at least partly, due to the broad power spectrum of the forcing and the nonnegligible memory of the SST. As shown in a stable linear system (appendix A), with a finite memory, the forced response has different phase shifts in response to different frequency components of the forcing. Therefore, for a forcing with a broad spectrum, there is no longer a single lag at which the forced response can achieve a perfect correlation with the forcing, resulting in an underestimation in the statistical assessment. The underestimation is more severe if the forcing has a broader spectrum and the forcing frequencies are higher; the broader spectrum leads to a larger phase difference of the response and the higher frequency makes the local memory relatively more important. Thus, the more systematic underestimation of the statistical assessment for interannual than decadal variability may be caused by a shorter time scale of the former, at which the SST memory is still not negligible. The more severe underestimation of the interannual variability of the North Atlantic impact than the tropical Pacific impact may also be understood, because the model tropical Pacific interannual ENSO forcing is dominated by a relatively narrow peak around 3–5 yr (Liu et al. 2000), while the North Atlantic SST interannual variability has no dominant peak (not shown).

5. The role of local ocean–atmosphere interaction and NAO

a. The role of local ocean–atmosphere coupling

The previous analysis suggests that the combined remote impact explains nearly half of the SSTA variance in the tropical Atlantic. This also implies that the other half of SST variability is independent of the remote forcing and therefore may be generated locally. This is

seen most convincingly in experiment PBC_TAV, in which substantial tropical Atlantic variability exists in spite of the absence of any remote SST influence. This is also consistent with an experiment in the COLA model (Huang et al. 2002), in which significant tropical Atlantic variability exists after the elimination of the Pacific impact. Here, we further show that this residual SST variability depends critically on local ocean–atmosphere coupling. We performed an additional sensitivity experiment PC_G, in which the PC is applied to over the entire global ocean (Table 1). The major difference between PC_G and PBC-TAV is therefore the additional suppression of local ocean–atmosphere coupling over the tropical Atlantic. The SSTA variance is now reduced by another 30%–40% (Figs. 6d,h compared with Figs. 6c,g). This experiment may be interpreted as the importance of local ocean–atmosphere coupling to TAV. It should however be noticed that our PC scheme may overestimate the effect of local coupling. First, the PC scheme decouples completely even the thermal ocean–atmosphere interaction (Barsugli and Battisti 1998). Second, the variance of the model atmospheric internal variability is weaker than in reality, likely due to the coarse model resolution. For example, the variance of the 500-mb geopotential height anomaly in the model is about half that in the National Centers for Environmental Prediction (NCEP) observation (not shown).

To further demonstrate the importance of local variability, we show that all the leading REOF modes of the full SSTA (in observations and CTRL) are well maintained in the residual SSTAs that are obtained after the removal of remote impacts. First, we consider the residual SSTAs derived from the statistical assessment (3.2). We will take as an example the tropical Pacific impact on total variability, which has the leading REOF modes as shown in Fig. 1. At each point in the tropical Atlantic, the impact of the tropical Pacific SST is extracted by regressing the seasonal SSTA with the seasonal TP-SST index at the lag of maximum correlation [as in (3.2)]; this remote impact is then removed from the SSTA to yield the residual SSTA. The 10 leading REOF modes of this residual SSTA field can be taken as the leading REOF modes after the removal of the tropical Pacific impact. For each REOF mode of the full SSTA, the “most similar” REOF mode in the residual SSTA is identified as the one with the highest pattern correlation. In both observations and the model, each leading REOF mode of the full SSTA (Fig. 1) is found to have a most similar REOF mode that stands out in the residual SSTA with virtually an identical pattern. The averaged pattern correlation coefficients of the most similar REOF modes for the four leading REOF modes of the full SSTA are over 0.98 for the total variability in observations and the FOAM CTRL (circle in Figs. 7a and 7b, respectively). Furthermore, the order of the most similar REOF modes remains the same in the residual SSTA as in the full SSTA. This suggests that

² The higher dynamic assessment of the extratropical Atlantic impact may also be contributed to partly by our PC scheme. The prescribed SST is blended with the model SST linearly from latitude 25° to 30° in both hemispheres. This may suppress some SST variability between 25° and 30°. However, this suppression effect is the same across all the time scales. Since decadal variability has a comparable North Atlantic impact in both assessments equatorward of 25°, this bias is unlikely to be the dominant cause for the difference of interannual variability of the two assessments for interannual variability.

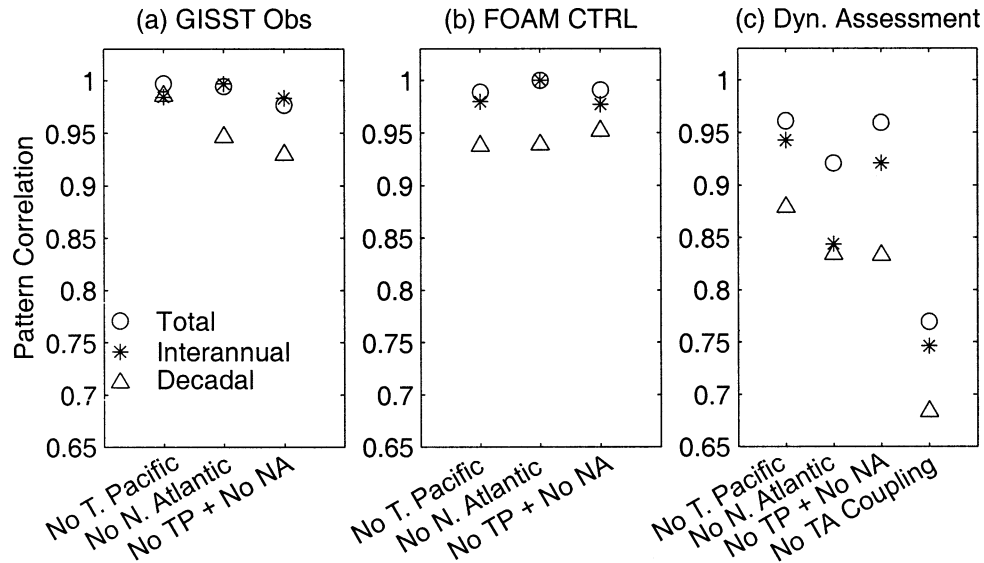


FIG. 7. Averaged pattern correlations between the four leading REOFs of the full SSTA and their most similar REOFs of the residual SSTA. The averaged pattern correlation is calculated as: $S = (\sum_{n=1}^4 \sqrt{u_n v_n} |c_n|) / (\sum_{n=1}^4 \sqrt{u_n v_n})$, where u_n and v_n are the explained variances of the n th REOF mode of the full SSTA and its most similar REOF mode of the residual SSTA, respectively, and c_n is the pattern correlation between the two. Circles, asterisks, and triangles are for total, interannual, and decadal variability, respectively. Statistical assessment of the (a) GISST observation and (b) the FOAM CTRL; (c) dynamic assessment of the model. The labels at the bottom show the cases of the residual SSTA. The first three are the cases after the removal of the impact of the tropical Pacific, North Atlantic, and the combined tropical Pacific/North Atlantic. In (c), the fourth case is for the sensitivity experiment PC_G, representing the dynamic assessment with neither remote impact nor local ocean–atmosphere coupling.

after the removal of the tropical Pacific impact, the dominant modes of total SST variability remain almost the same in the tropical Atlantic, except for a reduction of the variance. Similarly, the averaged pattern correlations are over 0.98 for interannual variability (asterisk) and over 0.93 for decadal variability (triangle) in observations (Fig. 7a) and the model (Fig. 7b). A similar conclusion can be obtained after the removal of the North Atlantic influence and the combined tropical Pacific and North Atlantic influence (Figs. 7a,b) (in the case of model decadal variability, the order of the leading REOF modes are slightly changed after the North Atlantic SST influence is removed). Based on the statistical analysis, we conclude that all the leading REOF modes are likely to be generated locally within the tropical Atlantic climate system, because they are little distorted by remote impacts. This appears to be consistent with previous studies, which suggested that the tropical Atlantic ocean–atmosphere system is able to generate substantial climate variability through local ocean–atmosphere coupling (Chang et al. 1997). Therefore, the main effect of the remote impact is to enhance the amplitude of the variability, rather than to generate new modes of variability in the tropical Atlantic.

A similar conclusion seems to hold in the model using the dynamic assessment. Now, the SSTAs of experiments PC_TP, PBC_ET, and PBC_TAV are used as the residual SSTAs after the removal of the tropical

Pacific impact, the extratropical Atlantic impact, and the combined tropical Pacific/extratropical Atlantic impact, respectively. The averaged pattern correlation coefficients are generally over 0.9 for total and interannual variability, and above 0.83 for decadal variability (Fig. 7c). The order of the leading REOF modes are changed somewhat. Figure 8 shows some examples in the case of interannual variability. The top four leading REOF modes of the full interannual SSTA (Fig. 8a)³ are similar to those of the total variability (Fig. 1b). All these REOF modes can be identified with the most similar REOF modes in the SSTAs of PC_TP (Fig. 8b), PBC_TP (Fig. 8c), and PBC_TAV (Fig. 8d), with the pattern correlations of about 0.9 and with some changes of the ranking of the REOFs. Therefore, as in the statistical assessment, the existence of the leading REOF modes are largely independent of the remote impact, while the variance the modes can be enhanced by the remote forcing.

These leading SST modes, however, appear to depend more critically on local ocean–atmosphere coupling. This can be seen in the REOF modes in PC_G (Fig. 8e), which can be taken as the residual SSTA with the de-

³ As for the total variability in Figs. 1b1 and 1b3, the spurious REOF2, which is loaded in the western equatorial Atlantic, is not shown here because it is caused by the deficient model equatorial seasonal cycle.

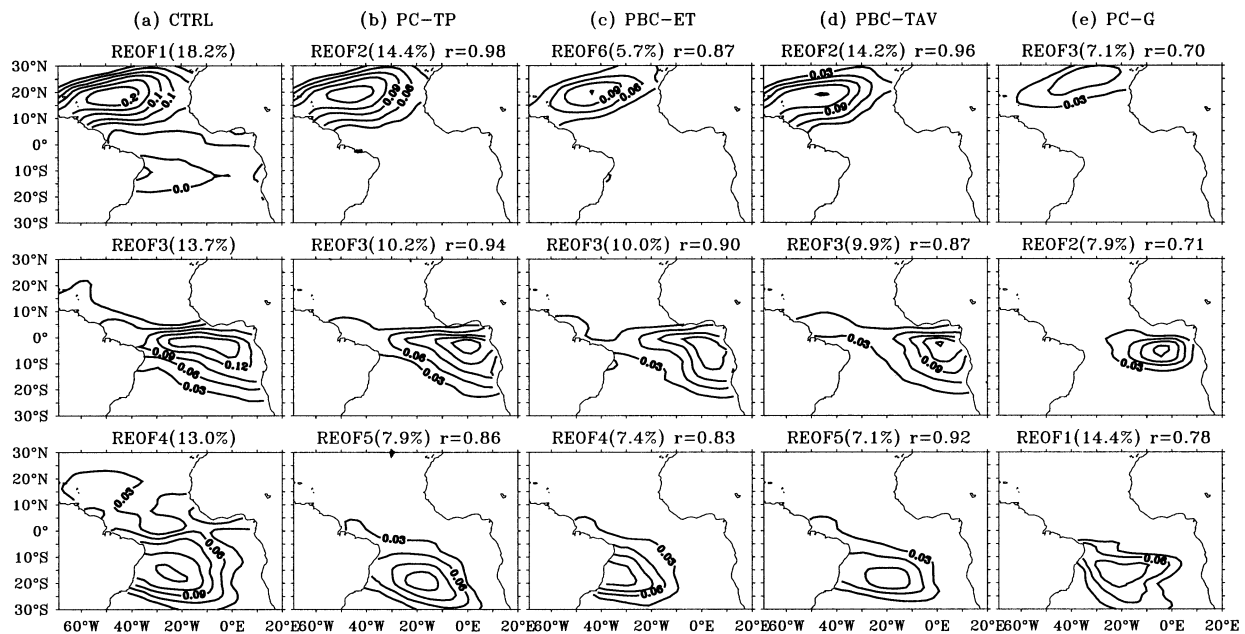


FIG. 8. REOF SST modes of interannual variability in the model. (a) The three leading REOF modes in CTRL (except the spurious REOF2 mode, see caption of Fig. 1). (b) The REOF modes that are “most similar” to the CTRL (top) REOF1, (middle) REOF3, and (bottom) REOF4 in PC-TP. For a particular CTRL REOF mode, the “most similar” REOF mode in PC-TP is chosen as the one with the maximum pattern correlation in all 10 REOF modes. (c), (d), (e) The same as (b) but for PBC_ET, PBC_TAV, and PC_G, respectively. For each REOF of the residual SSTA [panels (b)–(e)], the pattern correlation coefficient c with the corresponding REOF of the full SSTA is also given.

coupling of local ocean–atmosphere interaction as well as the removal of the remote impact. Now, in addition to the dramatic reduction of the variance as discussed in Table 1, the patterns of the corresponding REOF modes are also changed rather significantly, with the averaged pattern correlations dropping to about 0.75 for total and interannual variability and to 0.68 for decadal variability (Figs. 7c and 8e). Therefore, relative to the remote impact, local ocean–atmosphere coupling appears to play a more important role in determining the temporal–spatial structures of the leading REOF modes.

b. Remote impact of NAO

The remote impact of North Atlantic is so far assessed only in terms of its SST effect. In the statistical assessment, we have used the averaged North Atlantic SSTA as the forcing index, while in the dynamic assessment, only the SSTA in the North Atlantic is suppressed. The choice of the SSTA as the index makes the comparison of the two assessments more convenient. However, the impact of the North Atlantic SSTA could differ substantially from that of the classical NAO, which is defined in terms of the anomalous sea level pressure (SLP; Hurrell 1995) and therefore is likely to include a stronger component of atmospheric internal variability. Figure 9 shows the correlation of the NAO index and the Atlantic SSTA in observations and the model. The observation is dominated by a tripole structure predominantly north of the equator (Fig. 9a), as in

previous studies (e.g., Marshall et al. 2001). This tripole structure is well simulated in the model (Fig. 9b). The explained variances reach up to 20% in the tropical North Atlantic for interannual (Figs. 10a,c) and decadal (Figs. 10b,d) variability. This NAO impact differs substantially from that of the NA-SSTA (Figs. 4c,d), because the NAO index and NA-SSTA has a correlation less than 0.2 (as seen in Figs. 9a,b).

It remains difficult to assess the impact of NAO on TAV, because the NAO is dominated by the atmospheric internal variability. In experiment PBC_TAV, in spite of the elimination of the remote impact from the extratropical Atlantic SSTA, it remains possible that substantial SST variability in the tropical Atlantic (Figs. 6c,g) is caused by atmospheric internal variability over the North Atlantic atmospheric system, similar to the extratropical atmospheric bridge effect discussed in the North Pacific by Barnett et al. (1999) and Vimont et al. (2001). This effect of the NAO atmospheric variability can not be ruled out from our PC sensitivity experiments dynamically. Nevertheless, we can try to estimate the NAO effect with the statistical assessment. The correlation of the NAO index and Atlantic SSTA shows a tripole pattern in PBC_TAV (Fig. 9e), as in CTRL (Fig. 9b). Over the tropical North Atlantic, however, the correlation coefficient is less than 0.3, corresponding to an explained variance of less than 10%, similar to the case of CTRL. This suggests that the North Atlantic atmosphere internal variability contributes less than 10% of

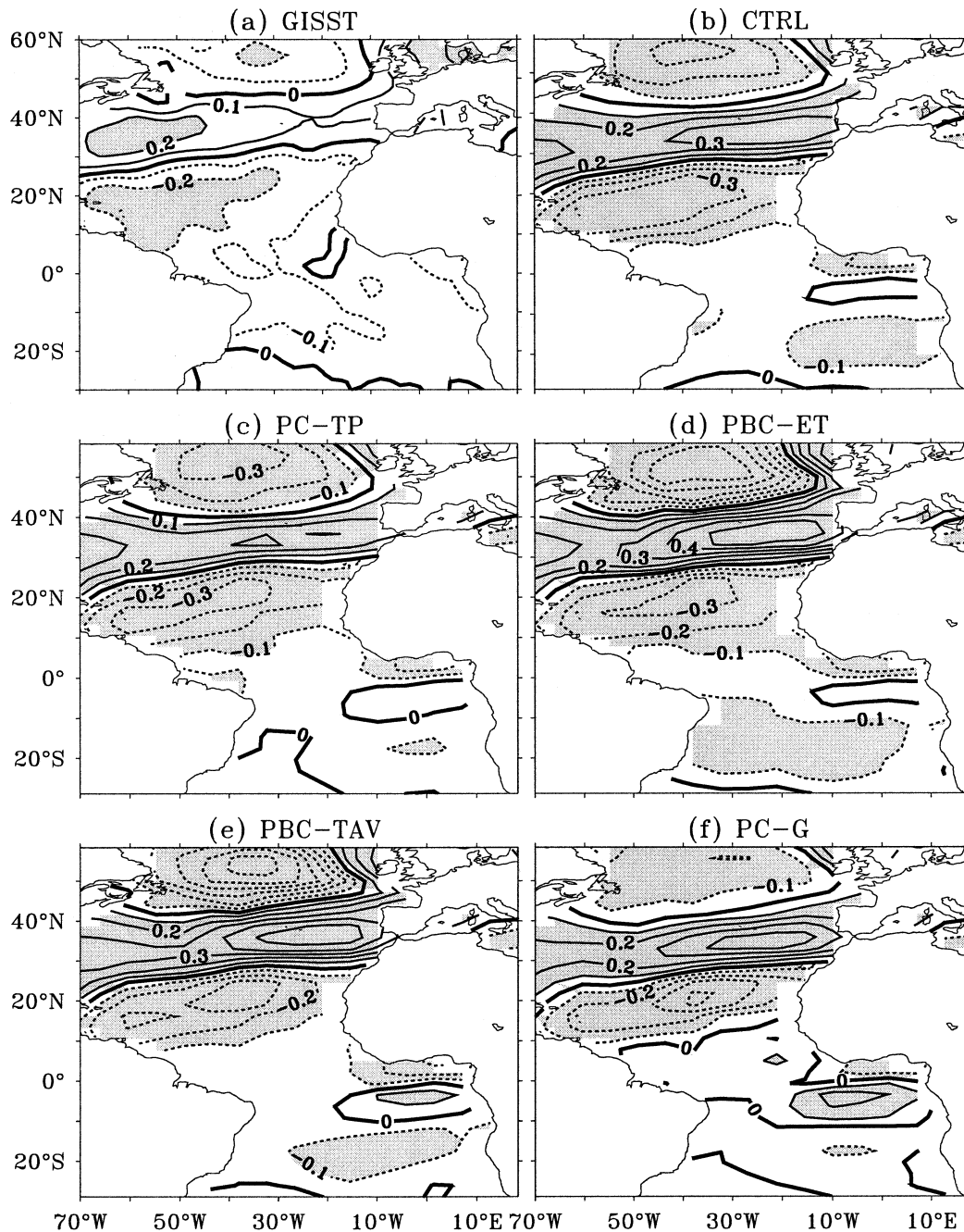


FIG. 9. Correlation between the NAO index and tropical Atlantic SSTA in (a) observations and (b)–(f) FOAM experiments. The NAO index is defined as the difference of the sea level pressure between Stykkisholmur, Iceland (about 40°N, 10°W) and Lisbon, Portugal (about 62°N, 20°W) (Hurrell 1995). The observation used the COADS sea level pressure and the correlation is done using the data of 1945–93. Shading convention as in Fig. 3.

the tropical North Atlantic SSTA in PBC-TAV. The minor effect of the NAO on tropical Atlantic SSTA is consistent in all the sensitivity experiments (Figs. 9c,d,f). This may suggest that, regardless of the remote impact and local ocean–atmosphere coupling, NAO and extratropical atmospheric internal variability may not

play a dominant role in forcing tropical Atlantic SST variability. However, one should be cautious about this conclusion. Partly, the NAO forcing and NA-SST forcing does show very similar features, such as the absence of impact south of the equator. Also, the statistic assessment may severely underestimate the impact on

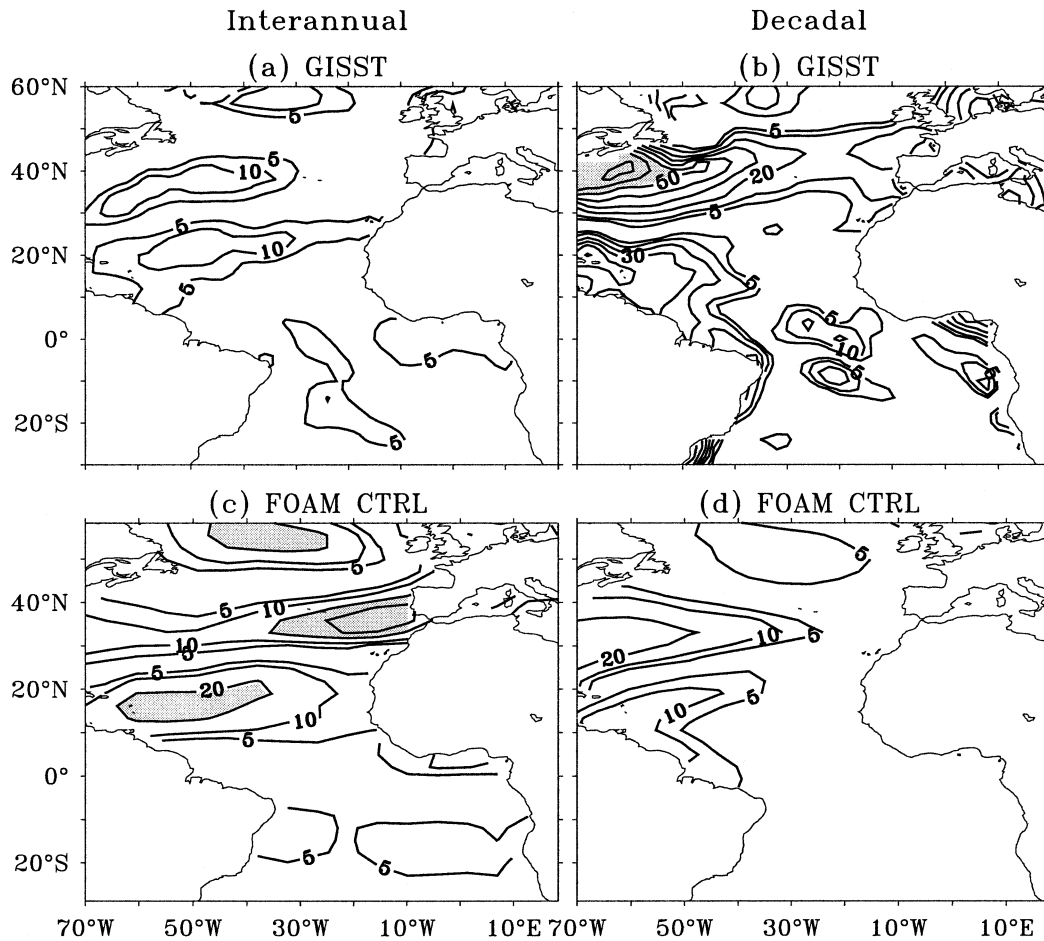


FIG. 10. Statistical assessment of the explained variance (%) by the NAO index on the Atlantic SST for (a), (c) interannual and (b), (d) decadal variability in (a), (b) observations and (c), (d) the CTRL simulation. The contour interval is 10 with the additional contour of 5 also plotted. Shading convention as in Fig. 4.

tropical Atlantic SSTA by NAO. This follows because, the NAO index, being taken from an atmospheric variable, has a very white spectrum at interannual to interdecadal time scales. As a result, the NAO index (or its bandpassed index) has a very flat power spectral band. The remote effect of this type of broadband index, as discussed in appendix A, may be severely underestimated using the statistical assessment.

6. Summary and discussion

Remote impact of tropical Pacific and North Atlantic SST variability on the tropical Atlantic SST variability is assessed using a traditional statistical method as well as a model-aided dynamic method. Overall, the two assessment methods suggest a consistent estimate: nearly half of the SSTA variance in the equatorial and tropical North Atlantic is caused by the remote impact. In spite of the significant remote impact, our study also suggests that local ocean–atmosphere coupling within the tropical Atlantic plays an important role in generating SST

variability. Thus, the nature of tropical Atlantic SST variability can be described as follows: the major modes of SST variability are generated internally within the tropical Atlantic climate system, and are then enhanced significantly by the remote impact from the tropical Pacific and extratropical Atlantic SST forcing.

This work is the first attempt to use the model-aided dynamic assessment. The comparison of the dynamic and the traditional statistical methods suggests that the statistical assessment tends to underestimate the remote impact on SST variability modestly for interannual variability. There are also regions near the equator where the remote impact tends to suppress, rather than to enhance, the SST variability. Furthermore, decadal variability tends to show more complex responses to the remote impact, implying mechanisms perhaps more complex than a linear passive response to remote forcing.

The model-aided dynamic assessment, in principle, should give the best estimate of the remote impact in the model climate. The extent to which the dynamic

assessment applies to the real world depends on the quality of the model simulation. Here, our model is reasonable in simulating the SST variability in the tropical North Atlantic, and, to a lesser degree, in the equatorial Atlantic. Therefore, conclusions from our dynamic assessment may also have implications for the real world in these regions. Our model is deficient in simulating the remote tropical Pacific and North Atlantic impact on the tropical South Atlantic and therefore we are cautious about our model assessment there.

The remote impact of extratropical South Atlantic SST can also be analyzed statistically and dynamically (Tables 1a,b,c, column 5), as was the North Atlantic SST forcing. The statistical assessment of observations shows a South Atlantic impact substantially weaker than the North Atlantic SST for interannual variability, but roughly comparable for decadal variability, while the statistical assessment of the model shows little South Atlantic impact for interannual variability but an impact comparable with that in observations for decadal variability. The dynamic assessment of the South Atlantic impact is roughly comparable with the dynamic assessment of the North Atlantic impact, both being much stronger than the corresponding statistical assessment. These results, however, should be taken with great caution, because of the poor quality of data and the very deficient model simulation there.

This work has left many important questions unanswered. First, the robustness of our dynamic assessment needs to be reassessed with improved models, particularly for the South Atlantic. Second, the differences between the dynamic and statistical assessment methods remain to be understood. Since the statistical assessment is limited by its linear statistical assumptions that are unlikely to be always true in the real world or a coupled model, the difference between the two assessments may shed light on the dynamic nature of the remote impact. For example, the overall consistency of the two assessments, as is the case of interannual variability forced by the tropical Pacific SST, may imply a largely passive response to the remote forcing. In addition, the negative remote impact in the dynamic assessment, which is impossible to identify statistically, may imply certain unknown dynamics of the local climate variability and the remote impact. This effect, although not dominant for the tropical Atlantic, especially, at shorter time scales, could be important for other climate variability. Finally, the response of the sensitivity experiments used for the dynamic assessment also needs to be better understood. The role of each teleconnection bridge due to the atmosphere, the ocean, and the coupled ocean–atmosphere process, needs to be clarified. The mechanism of local ocean–atmosphere coupling also needs to be better understood. Nevertheless, our study, together with previous studies (Liu et al. 2002; Wu and Liu 2002; Wu et al. 2002; Huang et al. 2002), demonstrates the potential of a coupled climate model as an important tool for our

understanding of climate variability and the assessment of the various remote impacts.

Acknowledgments. We would like to thank Dr. E. DeWeaver for a helpful discussion. This work is supported by NOAA, NASA, and DOE. The Chinese Academy of Sciences provided support under Grant ZKCX2-SW-210. The computation is carried at NCSA and NCAR.

APPENDIX A

A Simple Model Study

It is instructive to compare the statistical assessment with the dynamic assessment in a conceptual stochastic climate model (Frankignoul and Hasselmann 1977)

$$\frac{dT}{dt} = G(t) - \lambda T,$$

where $G(t) = F(t) + N(t)$ consists of a climate forcing $F(t)$ and a random noise $N(t)$ that is uncorrelated with the forcing, that is, $\langle F, N \rangle = 0$. The total response can be derived as

$$T(t) = \int_{-\infty}^t e^{-\lambda(t-s)} G(s) ds, \quad (\text{A.1})$$

and the response forced by F is

$$T_F(t) = \int_{-\infty}^t e^{-\lambda(t-s)} F(s) ds. \quad (\text{A.2})$$

The forced response (A.2) is identical to that from the dynamic assessment.

For the statistical assessment, the part of variability correlated with the forcing of lag τ is

$$T_s(t, \tau) = r(\tau)F(t + \tau), \quad (\text{A.3})$$

where $r(\tau) = \langle T, F(t + \tau) \rangle / \langle F, F \rangle$ is the lagged regression coefficient. The percentage of variance explained by $F(t + \tau)$ is therefore

$$\langle T_s, T_s \rangle / \langle T, T \rangle \equiv c^2(\tau),$$

where $c(\tau) = \langle T, F(t + \tau) \rangle / \sqrt{\langle F, F \rangle \langle T, T \rangle}$ is the lagged correlation coefficient. It is clear that, for a general forcing, there is no guarantee that the statistical estimate (A.3) extracts the true forced response (A.2).

Consider two simple cases of forcing. First, for a climate forcing of a single harmonic $F(t) = f \cos(\omega t)$, the forced response (A.2) is

$$T_F(t) = \frac{f \cos[\omega(t + l)]}{\sqrt{\lambda^2 + \omega^2}} = \frac{F(t + l)}{\sqrt{\lambda^2 + \omega^2}}, \quad (\text{A.4})$$

with $l = l(\omega)$ determined by

$$\begin{aligned} \cos(\omega l) &= \lambda / \sqrt{\lambda^2 + \omega^2}, \\ \sin(\omega l) &= -\omega / \sqrt{\lambda^2 + \omega^2}. \end{aligned} \quad (\text{A.5})$$

Here, $l < 0$, meaning a lagged response to the forcing. In the statistical assessment, with the ensemble average as the $M \rightarrow \infty$ limit of $\langle A(t), B(t) \rangle = 1/2M \int_{-M}^M A(t)B(t) dt$, the regression coefficient can be derived as $r(\tau) = \{\cos[\omega(\tau - l)]\}/(\sqrt{\lambda^2 + \omega^2})$ and the statistically extracted forced response (A.3) is

$$T_S(t, \tau) = \frac{\cos[\omega(\tau - l)]}{\sqrt{\lambda^2 + \omega^2}} F(t + \tau). \quad (\text{A.6})$$

Thus, the statistical assessment (A.6) extracts exactly the true response (A.4) if the lag is chosen ($\tau = l$) such that the lagged correlation is perfectly 1. This is easy to understand, because the forced response (A.4) evolves the same as the forcing except for a phase shift of l .

Next, consider a climate forcing with two harmonics of $\omega_1 \neq \omega_2$ as $F(t) = f_1 \cos(\omega_1 t) + f_2 \cos(\omega_2 t)$. With (A.4), the true forced response is now

$$T_F(t) = \sum_{n=1}^2 \frac{f_n \cos\{\omega_n[t + l(\omega_n)]\}}{\sqrt{\lambda^2 + \omega_n^2}}, \quad (\text{A.7})$$

with $l(\omega_n)$ determined as in (A.5). On the other hand, the statistically extracted solution can be derived similar to (A.6) as

$$T_S(t, \tau) = \frac{\sum_{n=1}^2 \frac{f_n^2 \cos\{\omega_n[\tau - l(\omega_n)]\}}{\sqrt{\lambda^2 + \omega_n^2}}}{\sum_{n=1}^2 f_n^2} F(t + \tau). \quad (\text{A.8})$$

Since in general $l(\omega_1) \neq l(\omega_2)$ as long as $\omega_1 \neq \omega_2$, the statistical extraction (A.8) can no longer recover the true forced solution (A.7). Furthermore, with (A.5), (A.7), and (A.8), one can show that the ratio of the variance of T_S is always smaller than that of T_F for any nonzero lag τ , that is

$$\Gamma(\tau) = \frac{\langle T_S, T_S \rangle}{\langle T_F, T_F \rangle} = \frac{\left[\sum_{n=1}^2 \frac{f_n^2}{\lambda^2 + \omega_n^2} (\lambda \cos \omega_n \tau - \omega_n \sin \omega_n \tau) \right]^2}{\left(\sum_{n=1}^2 f_n^2 \right) \left(\sum_{n=1}^2 \frac{f_n^2}{\lambda^2 + \omega_n^2} \right)} < 1. \quad (\text{A.9})$$

Thus, the statistical assessment always underestimates the forced response. This occurs because the phase shift (A.5) differs for different forcing frequencies. Therefore, it is impossible to have a single phase shift such that the statistical extraction can achieve a perfect correlation 1 with the forced solution. Nevertheless, the optimal extraction can still be achieved with the maximum correlation, usually with a negative τ , meaning the response lagging the forcing (not shown). Figure A1 shows two examples of the ratio $\Gamma(\tau)$ with $\omega_1 = 1$ for

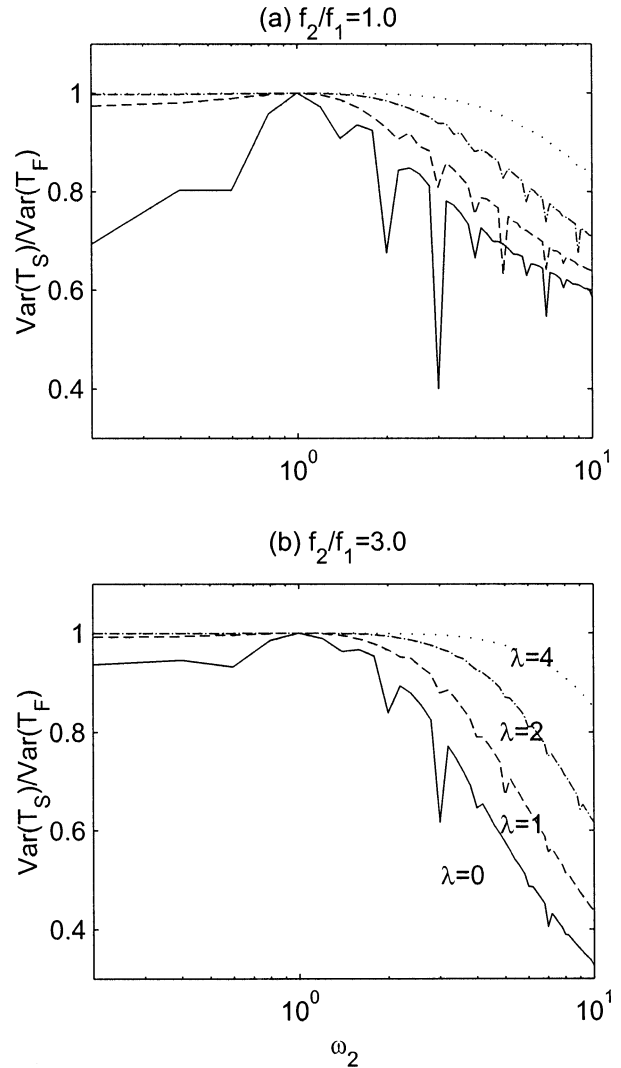


FIG. A1. The ratio of the variances of the forced response estimated from the statistical assessment T_S in (A.7) and the dynamic assessment (true solution) T_F in (A.6) in the simple model. The forcing has two harmonics with $\omega_1 = 1$ and (a) $f_2 = f_1$ and (b) $f_2 = 3f_1$. The variance ratio is shown as a function of ω_2 and for the damping coefficients $\lambda = 0$ (solid), $\lambda = 1$ (dash), $\lambda = 2$ (dash-dot), and $\lambda = 4$ (dot).

$f_2 = f_1$ (Fig. A1a) and $f_2 = 3f_1$ (Fig. A1b). The main feature is that the variance of the statistical assessment is underestimated more severely for a higher frequency ω_2 because of a broader forcing spectrum, and for a decreasing λ because of the increasing importance of the local variability term as the temporal memory. In the extreme case of very strong dissipation (or very slow variability) $\omega_n \ll \lambda$ ($n = 1, 2$), the memory term is negligible in (A.1) and we have $T \approx G/\lambda$. Now, even for a general forcing, the statistical method always recovers the true solution.

The simple model results are not directly applicable to realistic cases. Nevertheless, it has qualitative implications. The maximum correlation method tends to underestimate the forced response for a forcing of a

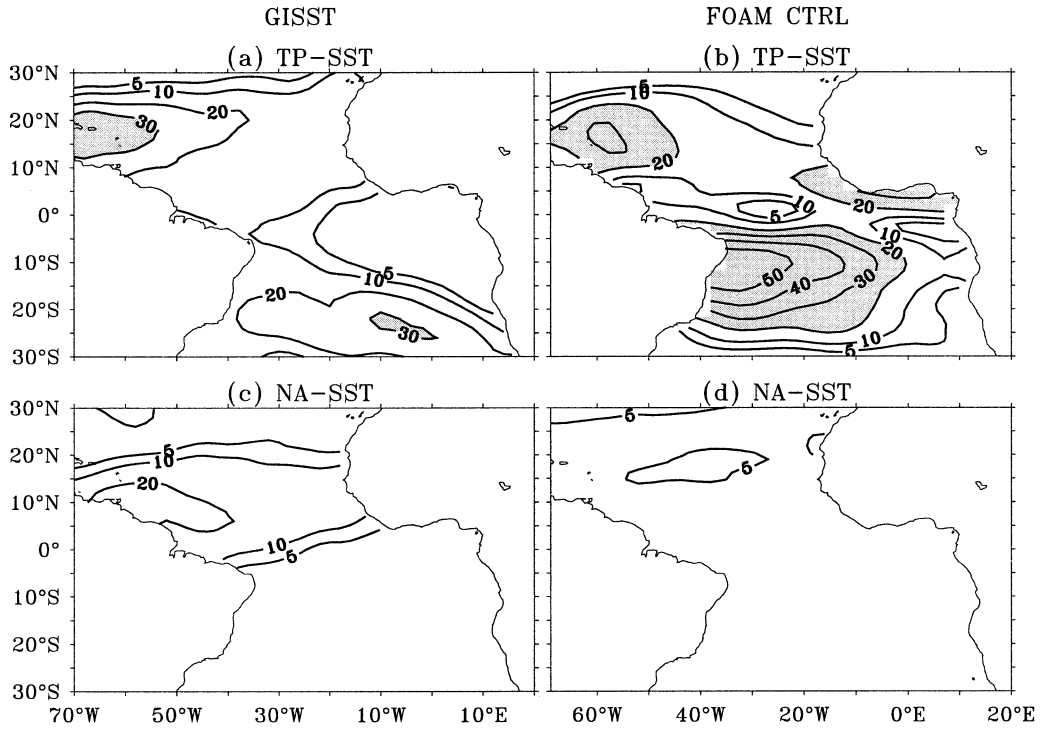


FIG. B1. Explained variance for interannual variability estimated using the single-lag correlation method of (3.1) for the (a), (b) tropical Pacific impact (with the tropical Atlantic lagging one season) and (c), (d) North Atlantic impact (zero lag) in (a), (c) observations and the (b), (d) FOAM CTRL. Shading convention as in Fig. 4.

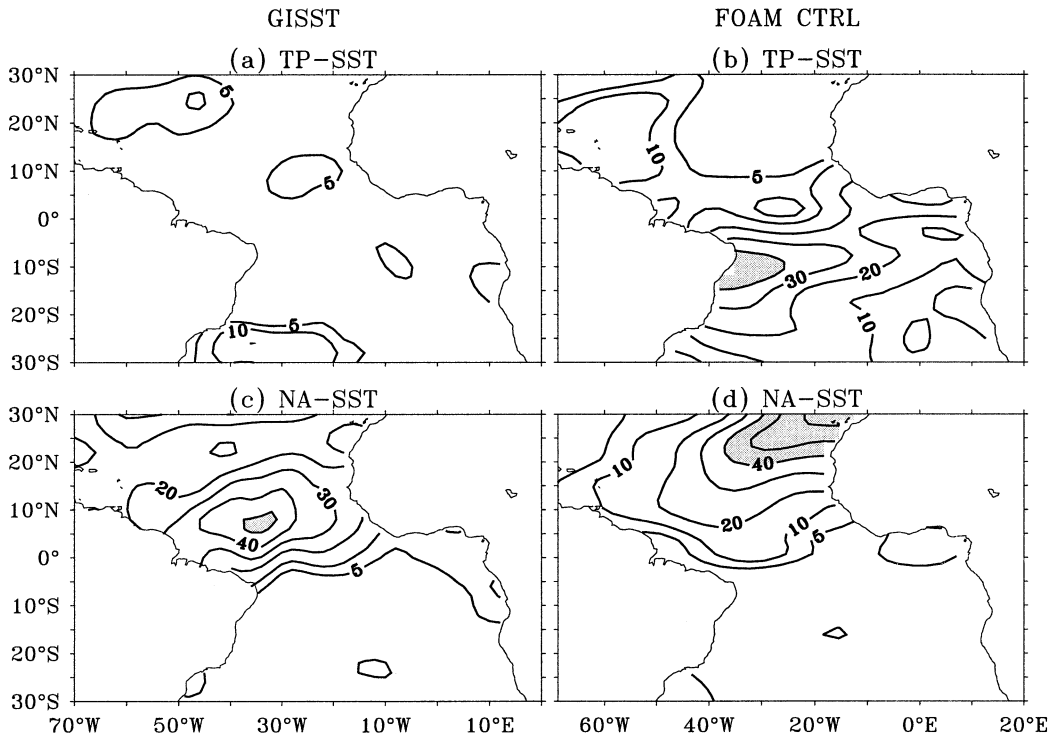


FIG. B2. The same as in Fig. B1 but for decadal variability.

broad spectrum and at time scales short or comparable with the local memory. For the extraction of SST variability, slow memory may still be effective at seasonal to interannual time scales and therefore the statistical assessment tends to be an underestimation, as in the case of FOAM here (Table 1a,b). It is also clear that the underestimation should not be a problem for atmospheric variables in monthly data because of the short memory of the atmosphere.

APPENDIX B

Additional Discussion of the Statistical Assessment

Figure 2 showed that the seasonal tropical Atlantic SSTA tends to lag the tropical Pacific SST by about 1 season, but tends to correlate simultaneously with North Atlantic SSTA. This lag relationship remains roughly similar for interannual variability (not shown). As a result, the remote impact estimated using the single-lag correlation (Fig. B1) resembles closely those from the pointwise maximum correlation (Fig. 4) for interannual variability.

The decadal variability has a wider range of lag for maximum correlation, especially for the observational tropical Pacific influence (not shown). This may partly reflect the noise of the statistics, because of the fewer realizations of decadal variability. It could also reflect a more complex dynamics of decadal variability than the interannual variability. The explained variance of the single-lag correlation (Fig. B2), however, is roughly similar to the pointwise maximum correlation estimate (Fig. 5). This appears to be attributed partly to the fact that the low-pass filtered data tends to show a lagged correlation oscillating with increasing lead/lag. Therefore, the maximum correlation is achieved after one-half or one cycle, which nevertheless is not much different from the simultaneous correlation.

REFERENCES

- Barnett, T., D. W. Pierce, M. Latif, D. Dommenges, and R. Saravanan, 1999: Interdecadal interactions between the Tropics and the mid-latitudes in the Pacific basin. *Geophys. Res. Lett.*, **26**, 615–618.
- Barsugli, J. J., and D. S. Battisti, 1998: The basic effects of atmosphere–ocean thermal coupling on midlatitude variability. *J. Atmos. Sci.*, **55**, 477–493.
- Boville, B. A., and P. Gent, 1998: The NCAR Climate System Model, version one. *J. Climate*, **11**, 1115–1130.
- Chang, P., L. Ji, and H. Li, 1997: A decadal climate variation in the tropical Atlantic Ocean from thermodynamic air–sea interaction. *Nature*, **385**, 516–518.
- Chiang, J. C., H. Y. Kushnir, and S. E. Zebiak, 2000: Interdecadal changes in eastern Pacific ITCZ variability and its influences on the Atlantic ITCZ. *Geophys. Res. Lett.*, **27**, 3687–3690.
- Covey, D. L., and S. Hastenrath, 1978: Pacific El Niño phenomenon and Atlantic circulation. *Mon. Wea. Rev.*, **106**, 1280–1287.
- Curtis, S., and S. Hastenrath, 1995: Forcing of anomalous sea surface temperature evolution in the tropical Atlantic during Pacific warm events. *J. Geophys. Res.*, **100** (C8), 15 835–15 847.
- Czaja, A., P. van der Vaart, and J. Marshall, 2002: A diagnostic study of the role of remote forcing in tropical Atlantic variability. *J. Climate*, **15**, 3280–3290.
- da Silva, A. M., C. C. Young, and S. Levitus, 1994: *Anomalies of Directly Observed Quantities*. Vol. 2, *Atlas of Surface Marine DATA 1994*, NOAA Atlas NESDIS 7, U.S. Department of Commerce, 416 pp.
- Davey, M., and Coauthors, 2002: STOIC: A study of coupled model climatology and variability in tropical ocean regions. *Climate Dyn.*, **18**, 403–420.
- Dawdy, D. R., and N. C. Matalas, 1964: Statistical and probability analysis of hydrologic data. Part III: Analysis of variance, covariance and time series. *Handbook of Applied Hydrology: A Compendium of Water-Resources Technology*, V. T. Chow, Ed., McGraw-Hill, 8.68–8.90.
- Enfield, D. B., and D. A. Mayer, 1997: Tropical Atlantic sea surface temperature variability and its relation to El Niño–Southern Oscillation. *J. Geophys. Res.*, **102C**, 929–945.
- , A. M. Mestas-Nunez, D. A. Mayer, and L. Cid-Serrano, 1999: How ubiquitous is the dipole relationship in tropical Atlantic sea surface temperature? *J. Geophys. Res.*, **104**, 7841–7848.
- Frankignoul, C., and K. Hasselmann, 1977: Stochastic climate models. Part II: Application to sea-surface temperature variability and thermocline variability. *Tellus*, **29**, 289–305.
- Hansen, D. V., and H. Bezdek, 1996: The nature of decadal anomalies in North Atlantic sea surface temperature. *J. Geophys. Res.*, **101**, 8749–8758.
- Hastenrath, S., 1978: On modes of tropical circulation and climate anomalies. *J. Atmos. Sci.*, **35**, 2222–2231.
- Houghton, R. W., and Y. M. Tourre, 1992: Characteristics of low-frequency sea surface temperature fluctuations in the tropical Atlantic. *J. Climate*, **5**, 765–771.
- Huang, B., P. S. Schopf, and Z. Pan, 2002: The ENSO effect on the tropical Atlantic variability: A regionally coupled model study. *Geophys. Res. Lett.*, **29**, 2039–2042.
- Hurrell, J., 1995: Decadal trends in the North Atlantic Oscillation: Regional temperatures and precipitation. *Science*, **269**, 676–679.
- Jacob, R., 1997: Low frequency variability in a simulated atmosphere ocean system. Ph.D. thesis, University of Wisconsin–Madison.
- Klein, S. A., B. J. Soden, and N.-C. Lau, 1999: Remote sea surface temperature variations during ENSO: Evidence for a tropical atmospheric bridge. *J. Climate*, **12**, 917–932.
- Latif, M., 2000: Tropical Pacific/Atlantic Ocean interactions at multi-decadal time scales. Max-Planck-Institut für Meteorology Rep. 305, 13 pp.
- , and T. Barnett, 1995: Interactions of the tropical oceans. *J. Climate*, **8**, 952–964.
- , and A. Grotzner, 2000: The equatorial Atlantic oscillation and its response to ENSO. *Climate Dyn.*, **16**, 213–218.
- Liu, Z., and L. Wu, 2000: Tropical Atlantic Oscillation in a coupled GCM. *Atmos. Sci. Lett.*, **1**, 26–36.
- , J. Kutzbach, and L. Wu, 2000: Modeling climatic shift of El Niño variability in the Holocene. *Geophys. Res. Lett.*, **27**, 2265–2268.
- , W. Wu, R. Gallimore, and R. Jacob, 2002: Search for the origins of Pacific decadal climate variability. *Geophys. Res. Lett.*, **29**, 1404, doi:10.1029/2001GL013735.
- , B. Otto-Bliessner, J. Kutzbach, L. Li, and C. Shields, 2003: Coupled climate simulation of the evolution of global monsoons in the Holocene. *J. Climate*, **16**, 2472–2490.
- Malanotte-Rizzoli, P., K. Hedstrom, H. Arango, and D. B. Haidvogel, 2000: Water mass pathways through the subtropical and tropical ocean in a climatological simulation of the North Atlantic ocean circulation. *Dyn. Atmos. Oceans*, **32**, 331–371.
- Marshall, J., and Coauthors, 2001: North Atlantic climate variability: Phenomena, impacts and mechanisms. *Int. J. Climatol.*, **21**, 1863–1898.
- Nobre, P., and J. Shukla, 1996: Variations of sea surface temperature, wind stress, and rainfall over the tropical Atlantic and South America. *J. Climate*, **9**, 2464–2479.
- Otto-Bliessner, B. L., and E. C. Brady, 2001: Tropical Pacific vari-

- ability in the NCAR Climate System Model. *J. Climate*, **14**, 3587–3607.
- Parker, D. E., C. K. Folland, A. Bevan, M. N. Ward, M. Jackson, and F. Maskell, 1995: Marine surface data for analysis of climate fluctuations on interannual to century time-scales. *Natural Climate Variability on Decadal to Century Time Scales*, D. G. Martinson et al., Eds., National Academy Press, 241–250.
- Ruiz-Barradas, A., J. Carton, and S. Nigam, 2000: Structure of interannual-to-decadal climate variability in the tropical Atlantic sector. *J. Climate*, **13**, 3285–3297.
- Saravanan, R., and P. Chang, 2000: Interactions between tropical Atlantic variability and El Niño–Southern Oscillation. *J. Climate*, **13**, 2177–2194.
- Seager, R., Y. Kushnir, M. Visbeck, N. Naik, J. Miller, G. Krahnmann and H. Cullen, 2000: Causes of Atlantic Ocean climate variability between 1958 and 1998. *J. Climate*, **13**, 2845–2863.
- Vimont, D. J., D. S. Battisti, and A. C. Hirst, 2001: Footprinting: A seasonal connection between the Tropics and mid-latitudes. *Geophys. Res. Lett.*, **28**, 3923–3926.
- von Storch, H., and F. W. Zwiers, 1999: *Statistical Analysis in Climate Research*. Cambridge University Press, 484 pp.
- Wu, L., and Z. Liu, 2002: Is tropical Atlantic variability driven by the North Atlantic Oscillation? *Geophys. Res. Lett.*, **29**, 1653, doi:10.1029/2002GL014939.
- , Q. Zhang, and Z. Liu, 2002: Searching for the role of ENSO in the tropical Atlantic variability. *Clivar Exchanges*, **7**, 20–24.
- , Z. Liu, R. Gallimore, R. Jacob, D. Lee, and Y. Zhong, 2003: Pacific decadal climate variability: The Tropical Mode and The North Pacific Mode. *J. Climate*, **16**, 1101–1120.
- Xie, S. P., and Y. Tanimoto, 1998: A pan-Atlantic decadal climate oscillation. *Geophys. Res. Lett.*, **25**, 1609–1612.
- Yang, J., 1999: A linkage between decadal climate variations in the Labrador Sea and the tropical Atlantic Ocean. *Geophys. Res. Lett.*, **26**, 1023–1026.
- Zebiak, S. E., 1993: Air–sea interaction in the equatorial Atlantic region. *J. Climate*, **6**, 1567–1586.
- Zhang, Y., J. M. Wallace, and D. S. Battisti, 1997: ENSO-like interdecadal variability: 1900–93. *J. Climate*, **10**, 1004–1020.